2011

Implementation of an Advanced Controller on a Torsional Mechanism

Chintan Trivedi
Cleveland State University

IMPLEMENTATION OF AN ADVANCED CONTROLLER

ON A TORSIONAL MECHANISM

CHINTAN TRIVEDI

BACHELOR OF ELECTRICAL ENGINEERING

SARDAR PATEL UNIVERSITY

June, 2007

Submitted in partial fulfillment of requirements for the degree

MASTER OF SCIENCE IN ELECTRICAL ENGINEERING

at the

CLEVELAND STATE UNIVERSITY

May, 2011

This thesis has been approved for the
for the Department of Electrical and Computer Engineering
and the College of Graduate Studies by

_____

Thesis Committee Chairperson, Dr. Lili Dong

_____

Department/Date

_____

Committee member, Dr. Hanz Richter

_____

Department/Date

_____

Committee member, Dr. Wenbing Zhao

_____

Department/Date

To my parents

and

my sister…

ACKNOWLEDGEMENTS

I would like to thank my advisor, Dr. Lili Dong for her support and guidance. I express my most sincere gratitude for her time and efforts. She has been a constant source of motivation and inspiration.

I would also like to thank Dr. Hanz Richter. His guidance in designing control systems and using Matlab was really helpful in conducting this research work.

Special thanks to Dr. Zhiqiang Gao for sharing his deep insights about a novel control methodology ADRC. I would also like to thank Dr. Wenbing Zhao for taking time out of his busy schedule and being on thesis committee.

I would also like to thank research students Gang Tian, Qinling Zheng, Kai Zhang, Yao Zhang and Prashanth Kandula for their intellectual input and helping me throughout the course of this research work.

I would also like to express my deepest gratitude to my parents and my sister Shraddha for providing me the encouragement and moral support.

IMPLEMENTATION OF AN ADVANCED CONTROLLER ON A TORSIONAL MECHANISM

CHINTAN TRIVEDI

ABSTRACT

The hardware implementation of an active disturbance rejection controller (ADRC) is presented in the thesis for a mechanical torsional plant. ADRC is a novel disturbance rejection control technique that is not completely dependent on mathematical models of physical systems. In ADRC framework external disturbances, system uncertainties, and internal dynamics of the system are estimated as a generalized disturbance by an extended state observer and the generalized disturbance is effectively canceled by a PD controller. A torsional plant represents a class of rotational systems. Its control challenges are the vibrations caused by mass imbalance, centrifugal imbalance, and the imbalance caused by the non-coincidence between the principal and geometric axes of rotating disc. In the thesis, the ADRC is applied to the torsional mechanism to control the angular speed and displacement of the rotating disc in the presences of the vibrations. Both simulation and hardware implementation results demonstrate the effectiveness of the ADRC. In addition, the hardware implementation results of the ADRC are compared with that of PD controller in terms of performance, control voltage requirement and tuning effort involved in the design process. The comparison study shows the superiority of the ADRC to PD controller.

TABLE OF CONTENTS

Page

LIST OF TABLES

Table **Page**

LIST OF FIGURES

Figure **Page**

ACRONYMS

ESO: Extended State Observer

POB: Perturbation Observer

PID: Proportional, Integral and Derivative

DOB: Disturbance Observer

UIO: Unknown Input Observer

HGO: High Gain Observer

ADRC: Active Disturbance Rejection Control

MEMS: Micro-Electro-Mechanical Systems

CHAPTER I

INTRODUCTION

1.1 Introduction

Torsional plant resembles dynamics of rotational systems. They have been used in a variety of industrial applications such as vehicle drive shafts, positioning systems of antenna and disk drives. The torsional plant has its unique system dynamics that presents its own challenges in its speed and position control. Details about the mechanism of torsional plant will be discussed in Chapter 2. In this section, the control problems associated with the plant are going to be discussed. The major control challenges of the plant are the vibrations caused by mass imbalance, centrifugal imbalance, and the imbalance caused by the non-coincidence between the principal and geometric axes of a rotating disc that is a part of the torsional mechanism. An Active Disturbance Rejection Controller (ADRC) is used to make the angular displacement of the rotating disc follow a desired displacement. The performance of ADRC will be compared with that of PD controller.

1.2 Existing Control Methods

Existing control design methods can be classified into two categories, i.e. classical control and modern control. Both methods are dependent on the mathematical model of the physical system to a certain extent. According to [1], most of the existing modern control methods are highly dependent on model information. However, in the real world, physical plants are highly nonlinear, time-varying and uncertain. In addition, external disturbances affect industrial processes. Modeling such systems in the presence of modeling uncertainties and external disturbances becomes either impossible or extremely difficult.

PID control, as a classical control method, has been very popular and has been employed in majority of industrial control applications since its first introduction in 1922 [2, 3]. Several modern control techniques have been developed since then. But PID control is still the most preferred choice of industrial engineers. What makes PID control technique so popular? It is its effectiveness in obtaining the desired control objective and its simplicity in hardware implementation in industrial control applications.

But with latest technological innovations, control task has continued to become more and more challenging and complex for a PID control and a need for other more capable control method has been identified. One of the major drawbacks of PID control is that it is a reactive controller. It only reacts to the feedback of the system and it has nothing to do with the internal states of the system. The reactive feature is a very fundamental limitation that affects the performance of the PID controller. The limitation results in the poor performance of PID controller in the presences of nonlinearities,

disturbances and system uncertainties. In addition, the controller parameters of the PID control have to be found by trial-and-error method. There is no universal rule to design the controller parameters for PID.

Modern control system can address the limitation of PID controller. But modern controllers have their own problems. The complexity involved in implementing the modern controller has prevented its widespread applications even after more than 40 years of their introduction in the literature. Nowadays 90% of industrial control processes use PID control as primary control method instead of a modern controller [4].

In the past several decades, theoreticians and practitioners have been trying to develop a control technique that is less trial-and-error-based, simple to implement, and not requiring accurate mathematical model of a system. Robust control is such a control solution that allows small uncertainties [5]. Other control solutions are based on disturbance estimators such as unknown input observer (UIO), disturbance observer (DOB), perturbation observer (POB) and extended state observer (ESO) [6].

Active disturbance rejection controller (ADRC) is a recently developed practical control methodology that requires only limited information of the model and is also as simple to implement as the PID controller. The only information it requires is the relative order of the physical system and controller gain. With only two parameters to tune, it is simple to be implemented [7].

1.3 State Observers

State observers estimate internal states of a plant using the real-time information of input and output of the plant. They are very useful in monitoring system dynamics, since the information state observers provide cannot be obtained by means of physical instruments. Design of state observers is based on mathematical model of the plant and it is usually presumed that the available model information is precise. However, in reality, the model cannot be accurate due to nonlinearities, model and parameter uncertainties and disturbances. These presumptions either make the performance of the state observer inferior to the desired performance or simply make the observer impossible to use. A brief survey of observers is presented below.

- Disturbance Observer (DOB): It uses binomial Q-filters, and only has one tuning parameter. The observer employs a model that is different from the plant but few guidelines are available on the design of observer. However, the effect of Q-filter on the observer's performance and its robustness has not been clarified [8]. The factors that make its implementation difficult are the additional efforts involved in designing a separate state observer and the risk to make system unstable.
- Unknown Input Observer (UIO): It is an observer that estimates internal states of the plant along with disturbances. The observer is based on a linear design model and disturbance model. The advantage of Unknown Input Observer over Disturbance Observer is that the controller and observer designs are completely independent of each other. Its performance limitation is that its accuracy is still dependent on the accurate mathematical model.

- High Gain Observer (HGO): It can also be used to estimate system dynamics and disturbances. But the high gain in observer makes the system very sensitive to noise.
- Perturbation Observer (POB): It has been proposed by several researchers in discrete state space form. However, the stability proof of POB has not been established and it requires detailed mathematical model of a physical system [9].

1.4 Active Disturbance Rejection Control

Active Disturbance Rejection Control (ADRC) was first developed by J. Han with nonlinear gains [10, 11]. Although successful, it was difficult to implement because of nonlinear gains. The number of gains required to be tuned was also very high. The nonlinear ADRC was modified with linearized gains and parameterized by Z. Gao in [12]. With parameterized gains, the ADRC became easy to implement in practice.

ADRC requires little information of the plant and it is not completely dependent on the mathematical model of the system which makes it very robust against system uncertainty [13]. It actively estimates all the states of plant from its input and output by means of an extended state observer (ESO). Model and parameter uncertainties and external disturbance are treated as a generalized disturbance. The generalized disturbance is then actively estimated and cancelled in real time with a PD controller. Once uncertainties and disturbances are estimated effectively, the plant is forced to act as a nominal plant, which is easier to control.

ADRC combines the best of both control paradigms, state observer from modern control and PID control from classical control. It is a complementary solution to prevailing control methodologies rather than a substitute. It has been successfully applied to a variety of industrial control problems that validate its effectiveness. It has also been designed and successfully implemented in both discrete and continuous forms [14]. Stability proof of ADRC in frequency domain has also been well established [15].

1.5 Contribution of Thesis

In this thesis, ADRC is successfully and originally implemented through using Matlab real-time workshop and Matlab Real-time windows Target toolbox for position control of a torsional plant.

These two toolboxes are used extensively for modeling, controller design and hardware implementation. Real-Time Windows Target has a set of I/O blocks that are used to create interface between simulation model and the physical I/O boards connected to actual torsional plant. After creating a simulation model of the system that includes controller and I/O blocks, hardware implementation is performed and simulation model is executed in real-time on actual torsional plant.

An integrated hardware and software environment for controller design and hardware implementation is presented in Chapters 3, 4, and 5. The environment enables fast controller design and allows users to observe its behavior on real physical system in real-time on windows based PC.

1.6 Organization of Thesis

The following part of the thesis is organized as follows. The dynamic modeling of an ECP torsional plant is discussed in Chapter 2, in which a torsional plant with one degree of freedom is modeled. Model validation and parameter tuning are also discussed in this chapter.

Details of designing ADRC are discussed in Chapter 3. In this chapter, the controller design process is explained for a second order motion control system.

Simulation results of ADRC on torsional plant are shown in Chapter 4. In Chapter 5, hardware implementation of ADRC on torsional plant is presented and the implementation results are compared with the ones for PID control. The ADRC shows advantages in performance and ease of tuning over PID controller. Concluding remarks and possible directions of future work are discussed in Chapter 6.

CHAPTER II

MODELING OF TORSIONAL PLANT

2.1 Introduction of Torsional Plant

Rotational systems are an important class of physical systems for which automatic controls are employed to control position and velocity. Rotational systems such as vehicle's drive shafts, the positioning system of antenna (to track satellites), and disk drives are modeled in a way that is very similar to modeling a torsional plant [16]. A controller that is designed and successfully implemented on a torsional plant can be readily implemented on other rotational systems. In this thesis, an advanced controller is developed on a torsional plant. The performance of this controller is compared to the one of PID controller which is widely used for position and speed control of above mentioned rotational systems.

Figure 1 shows an ECP torsional plant used in Control Systems Lab at Cleveland State University. The torsional plant has a vertical shaft, three disks and three incremental encoders. There is one encoder for each disk. Vertical shaft is torsionally flexible and is

suspended on anti-friction ball bearings. The shaft is driven by a brushless dc servo motor connected via a rigid belt and pulley system with a 3-to-1 speed reduction ratio. The encoder located on the base of the shaft measures the angular displacement of the disk. A torsional plant with one degree of freedom is used for controller design. The angular position of the bottom plate in Figure 1 will be driven to a desired position by the controller. By changing the position of brass cylinders mounted on the plate, total inertia of the system can be changed as well. The change of system' inertia will be helpful in examining the robustness of controller against system uncertainties.

2.2 Modeling of Torsional Plant

There are two methods which can be used for modeling physical systems. They are

- First Principles modeling;
- Empirical modeling.

First principles modeling is describing a system in mathematical equations by laws of physics. For the systems that are too complex to be defined by laws of physics, they are generally modeled by empirical method in which a system is treated as a black box and the modeling is dependent on the input-output relationship. In this thesis first principles modeling is used to model the torsional plant.

Figure 1: Photo of torsional plant

2.1.1 First Principles Modeling

To model rotational systems, Newton's laws of rotation are used. According to Newton's second law of rotation

$$T_L = J\ddot{\theta} + B\dot{\theta} \tag{2.1}$$

In (2.1),

T_L= Torque of load

J = Total inertia of system

B = Friction constant

$\ddot{\theta}$ = Angular acceleration

$\dot{\theta}$ = Angular velocity

The input voltage given to servo motor is *u(t)* that generates torque T_M which is

$$T_M = \text{Gain of servo amplifier} \times \text{Gain of motor} \times u(t) \quad (2.2)$$

Equation (2.2) can be rewritten as

$$T_M = K_{SA} \times K_M \times u(t) \quad (2.3)$$

In (2.3), K_{SA} is the gain of servo amplifier, and K_M is the gain of motor. To find the transfer function from input to output i.e. from input voltage *u(t)* to output angular position θ, the torque on motor side has to be converted to torque on plate side.

There is a speed reduction of 3 to 1 from motor to plate. The motor is rotating at a speed that is three-time the speed of the plate. With gear reduction, there are speed reduction and torque amplification of equal amount on the load side. So the torque on plate side (T_L) is three time the torque on motor side (T_M). Figure 2 shows speed reduction of 3 to 1 between motor and plate.

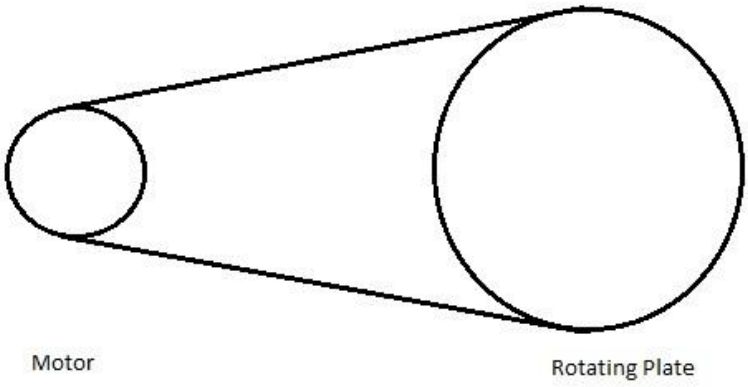

Figure 2: Relationship between motor and rotating plate

The relationship between the load torque T_L and motor torque T_M is shown in (2.4).

$$T_L = 3 \times T_M \tag{2.4}$$

Substituting (2.4) into (2.1) yields

$$3 \times T_M = J\ddot{\theta} + B\dot{\theta} \tag{2.5}$$

$$3 \times K_{SA} \times K_M \times u(t) = J\ddot{\theta} + B\dot{\theta} \tag{2.6}$$

In above differential equations, all parameters except friction constant B are known. The gain of servo amplifier (K_{SA}) and gain of servo motor (K_M) are constant, input voltage $u(t)$ is measured and total inertial J is calculated. The calculation of total initial (J_{Total}) is given by (2.7), where J_{plate} represents the inertia of plate, J_{Motor} represents the inertia of motor, and $J_{Cylinder}$ represents the inertia of cylinder.

$$J_{Total} = J_{Plate} + J_{Motor} + 2 \times J_{Cylinder} \tag{2.7}$$

$$= 0.0019 + 0.0005 + 2 \times 0.0009563$$

$$= 0.004312\ kg.m^2$$

The value of friction constant *B* can be found experimentally. Constant input voltage is given that makes the plate rotate at constant angular velocity resulting in zero angular acceleration. To find value *B*, we let the plate rotate at constant velocity of 500 *rpm*. From the torsional plant manual [17], we get the values for gain of servo amplifier as K_{SA}=1.5 *A/V* and gain of motor K_M=0.086. Input voltage *u(t)* is measured which is found to be 0.5 volts. The value of *B* is calculated through (2.8) and is found to be *B=0.00618.*

$$B = 3 \times K_{SA} \times K_M \times \frac{u(t)}{\dot{\theta}(t)} \tag{2.8}$$

Substituting the parameter values into (2.6), and conducting Laplace transform on (2.6), we can obtain the transfer function from input voltage to output position. The transfer function is

$$\frac{\theta(s)}{U(s)} = \frac{3K_{SA}K_M}{Js^2 + Bs} \tag{2.9}$$

$$\frac{\theta(s)}{U(s)} = \frac{0.387}{0.004312\,s^2 + 0.00618s} \tag{2.10}$$

The mathematical model of torsional plant is given by (2.9) and (2.10). Next we have to check whether the mathematical model is an accurate representation of the actual physical plant.

2.2 Model Validation

In the process of modeling a physical system, assumptions are generally made to reduce complexity of the modeling process. Model validation is an iterative process during which the developed mathematical model is calibrated and the output response of the mathematical model is compared to the one of actual physical system. Using the difference between real output and the output of mathematical model, we can adjust the model parameters till the output response with desired accuracy is obtained [18].

To validate the model developed for torsional plant, the output responses of mathematical model and physical plant are compared, and the model parameters inertia J and friction constant B are adjusted till desired output response is obtained from the model. A PID controller with identical controller gains is used to control the output of torsional plant and the output of mathematical model. By using identical controller gains, controller will have the same effect on mathematical model as it will have on the torsional plant. In Figure 3, a block diagram for model validation is shown. The plate of torsional plant is rotated at a constant angular velocity of 500 *rpm*. The output of mathematical model is compared with the output of real torsional plant.

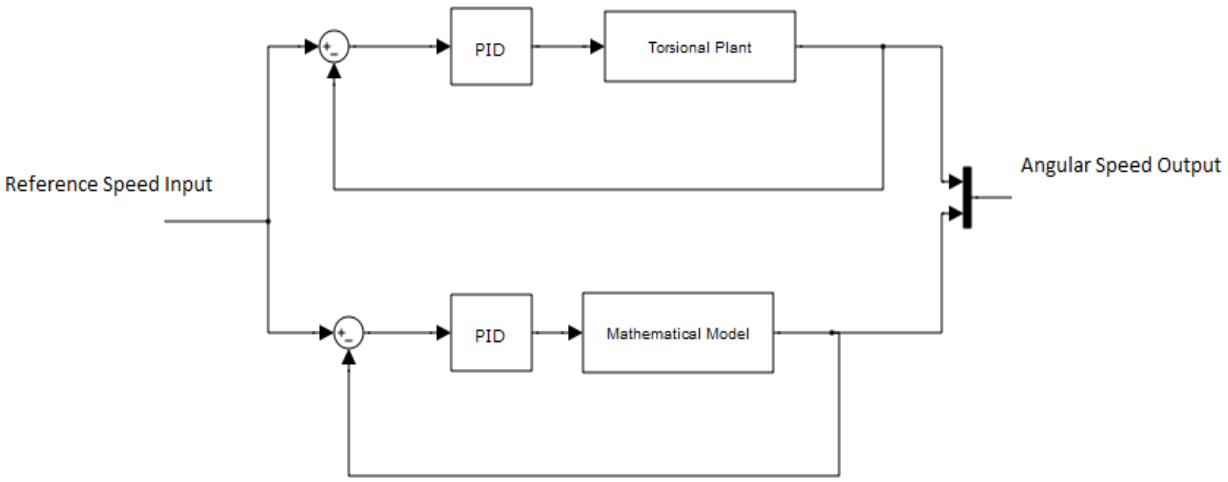

Figure 3: Block diagram of model validation

The system parameters of mathematical model are tuned so that the output response of the mathematical model matches the response of actual system. This process is completed iteratively by changing inertia and friction constant of the mathematical model. The differences in the actual and model response are caused by the assumptions made during the modeling process. Figure 4 shows the output responses of the mathematical model and actual torsional plant without tuned model parameters.

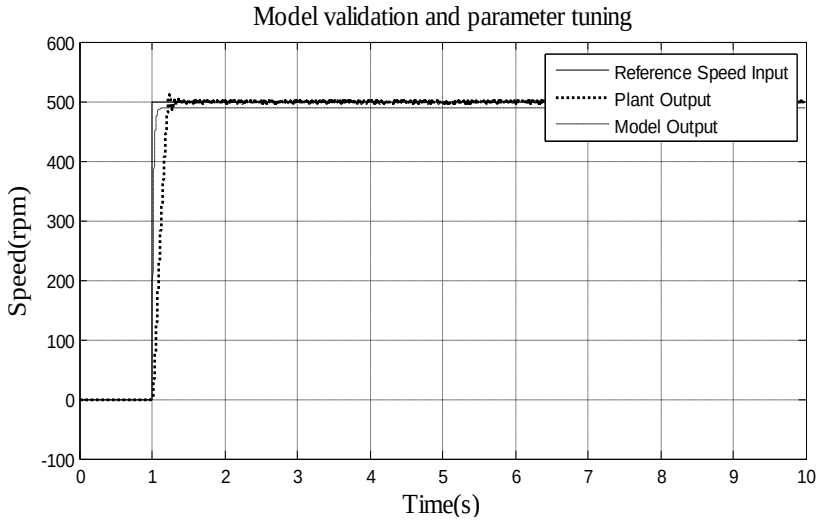

Figure 4: Output responses of the mathematical model and actual torsional plant

In Figure 4, the difference between two output responses caused by assumption is clearly observed. By tuning model parameters, i.e. inertia and friction constant, the model response can be improved and a response that is much close to the one of actual plant can be obtained.

Through understanding the effect of inertia and friction constant on the torsional plant, we could further simplify the tuning of system parameters. Changing the inertia results in the change in how fast the output reaches steady state value and changing friction constant results in the change in steady state value. From Figure 4, the output response of the mathematical model is faster than that of the actual torsional plant and the steady state value of the output of the mathematical model is less than that of torsional plant. To match the actual response, we have to increase the friction constant and inertia constant. After iterative tuning, the output responses with tuned system parameters are obtained as shown in Figure 5.

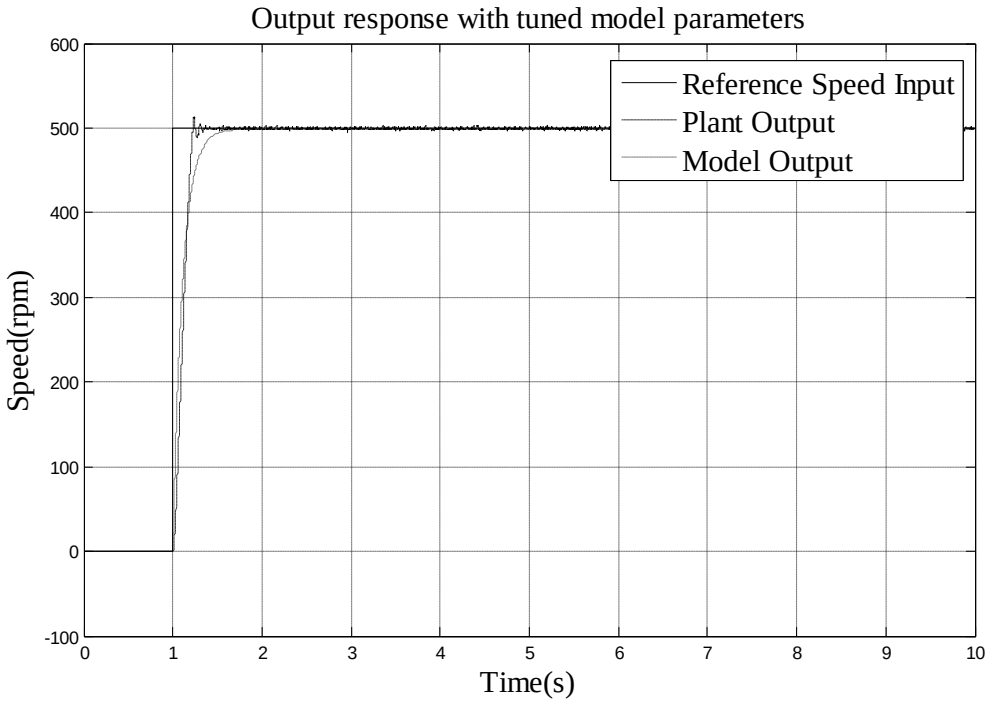

Figure 5: Output response with tuned model parameters

The calculated and tuned system parameters are listed in Table I.

TABLE I: PARAMETER VALUES FOR MODEL VALIDATION

Model	**Inertia (*J*)** $kg.m^2$	**Friction Constant (*B*)**	**Controller Gains**		
			K_p	K_i	K_d
Calculated	0.004312	0.00618	0.65	0.000007	0.0005
Tuned	0.02712	0.00078	0.65	0.000007	.0005

2.3 Summary of the chapter

The dynamic modeling of torsional plant is discussed in this chapter. Mathematical model of the torsional plant is developed using Newton's second law for rotational motion around a fixed axis. After model development, model validation is discussed in which fine adjustment to mathematical model parameters are made in order to remove any difference between mathematical model and actual torsional plant. This chapter provides foundation for controller design and implementation that is discussed in the next chapter.

CHAPTER III

APPLICATION OF ACTIVE DISTURBANCE REJECTION CONTROL TO TORSIONAL MECHANISM

3.1 Introduction to ADRC

Even after almost 90 years since PID controller was first introduced to industry by Minorsky in 1922, as high as 90% of industrial control applications today still use the controller to control physical processes. The PID controller is not only effective but simple to understand and implement. That's why it remains so popular for such a long time. It is therefore important to understand what makes a PID controller effective.

PID is an error based control design that focuses on minimizing and eliminating the tracking error between a reference input and measured output. If r is the reference input that the output (y) of a physical process has to follow, the control law will have to be designed in such a way that the tracking error $e = r - y$ is zero ideally, or as small as possible [19]. By obtaining past, present and the trend of immediate future of error, appropriate control action should be taken that responds to each of the error term. The formula of this PID controller is given by (3.1), where k_p denotes the proportional gain, k_I represents integral gain, and k_D represents the derivative gain.

$$u = k_p e + k_I \int e + k_D \dot{e} \tag{3.1}$$

The desired performance of PID is obtained by adjusting the values of k_P, k_I and k_D in (3.1). From the first introduction of PID to industry, a number of improvements have been made in gain tuning process such as automatic gain scheduling and Ziegler-Nichols tuning method. Nevertheless, the tuning process of PID controller is still trial-and-error based.

Another control methodology is model based control design such as pole-placement control for linear time invariant systems and feedback linearization method for nonlinear systems. In model based control, a major assumption is made that the mathematical model is an accurate expression of physical plant. However, for some nonlinear and time varying systems like the motion control system, the hysteresis in motor dynamics and backlash in gearboxes are difficult to describe mathematically with great accuracy.

ADRC was a practical solution designed to address the difference between mathematical model and actual physical plant. It became a solution that is complementary to existing control methods. The ADRC uses state observer from the modern control theory for improved performance. It also has the simplicity of PID controller for easy implementation. It is neither highly model dependent, nor completely trial-and-error based. But it is very effective in obtaining desired performance.

ADRC was first formulated as a nonlinear controller with nonlinear gains [20]. However, implementing the ADRC with nonlinear gains was a very challenging task because of its multiple nonlinear gains to be tuned. To simplify the implementation and

tuning of ADRC, gains were linearized and the number of parameters to be tuned was reduced. In its linearized form, ADRC has only three parameters to be tuned for performance improvement. They are observer bandwidth ω_o, controller bandwidth ω_c and controller gain b_0. Three-parameter tuning feature simplified the implementation and tuning process of ADRC to a great extent. It results in the successful implementation of ADRC for wide variety of applications such as motion control [21-23], chemical process control [24], web tension regulation [25], power systems [26], vibrational MEMS gyroscope [27, 28]. Successful implementation of ADRC is not limited to Single-Input-Single-Output systems. It has also been successfully applied to other complex and multi-input-and-multi-output systems like turbofan engine [29].

From (2.10), we can see that the torsional plant is a second-order system. For a second order motion (position) control system, the mathematical expression that relates system input *u(t)*, position output *y(t)* and external disturbance *w(t)* can be given by

$$\ddot{y}(t) + a_1\dot{y}(t) + a_2 y(t) = bu(t) + w(t) \tag{3.2}$$

In (3.2), a_1, a_2, and b are coefficients of the differential equation.

ADRC design for above mentioned motion control system can be explained by transforming the control problem into disturbance rejection framework. If modeling uncertainty, internal dynamics and external disturbance can be actively estimated in real-time, the plant will be reduced to a simplified plant that can be controlled by a PD controller. In a disturbance rejection framework the motion control system can be described as (3.3) and (3.4), where $f(y, \dot{y}, \omega, t)$ or represented by "*f*" includes internal

dynamics and external disturbance. The term *f* represents any input forces to the system excluding the control effort. We also define *f* as a generalized disturbance.

$$\ddot{y}(t) = bu(t) + w(t) - a_1\dot{y}(t) - a_2 y(t) \tag{3.3}$$

$$\ddot{y}(t) = f(y, \dot{y}, w, t) + bu(t) \tag{3.4}$$

3.2 Controller Design

The control task can be divided into a two step process:

- Estimating *f* using an extended state observer (ESO)
- Designing control law and tuning gains

ESO requires the least amount of plant information compared to all other observers used for state estimates and it only has one tuning parameter. These features make the ESO very easy to implement in real world and robust against model uncertainties. The effectiveness of ADRC is dependent on the accurate estimations of system dynamics and disturbances with ESO.

Design of ESO for a second order motion control system is shown as follows. System dynamics and disturbances are treated as generalized disturbance and estimated with an augmented state which makes the third-order state for ESO.

For (3.4), we choose $x = \begin{bmatrix} x_1 \\ x_2 \\ x_3 \end{bmatrix}$, where $x_1 = y, x_2 = \dot{y}, x_3 = d,$ and d=f. We suppose f (d) is differentiable and the derivative of f (d) is bounded within the domain of interests. Then we can write the state-space model of (3.4) as

$$\dot{x} = Ax + Bu + E\dot{d} \tag{3.5}$$

$$y = Cx \tag{3.6}$$

In (3.5) and (3.6), we have

$$A = \begin{bmatrix} 0 & 1 & 0 \\ 0 & 0 & 1 \\ 0 & 0 & 0 \end{bmatrix} B = \begin{bmatrix} 0 \\ b \\ 0 \end{bmatrix}, \quad E = \begin{bmatrix} 0 \\ 0 \\ 1 \end{bmatrix} \text{ and } C = [1 \quad 0 \quad 0].$$

The ESO based on (3.5) and (3.6) can be derived as,

$$\dot{z} = Az + Bu + L(y - \hat{y}) \tag{3.7}$$

$$\hat{y} = Cz \tag{3.8}$$

where $z = [z_1 \quad z_2 \quad z_3]^T$ is estimated state vector of x, $\hat{y}$ is an estimate of output y, L is gain vector of ESO and L=$[\beta_1 \quad \beta_2 \quad \beta_3]^T$. To locate all the eigenvalues of the ESO at -ω_o, the values of elements of the vector L are chosen as $\beta_i = \binom{3}{i} . \omega_0, i = 1,2,3$ [7]. With parameterization of ESO gains, β_1, β_2 and β_3, the only tuning parameter of ESO is

ω_o. After proper tuning, the estimates of *y*, derivative of *y*, and *f* are obtained which will be used to design the control law.

The control law is designed as (3.9).

$$u = \frac{u_0 - z_3}{b} \tag{3.9}$$

Suppose z_3 is an accurate estimation of *f*. Substituting (3.9) into (3.4), we will have

$$\ddot{y} = b\frac{u_0 - z_3}{b} + d \tag{3.10}$$

$$\approx (u_0 - d) + d$$

$$\ddot{y} = u_0 \tag{3.11}$$

From (3.11), we can see that the original second-order plant is simplified as a second-order integrator. For a pure integral plant, a PD control law can be used as

$$u_0 = k_1(r - z_1) - k_2 z_2 \tag{3.12}$$

In (3.12), k_1 and k_2 are proportional and derivative gains respectively, z_1 is an estimate of *y* , z_2 is an estimate of $\dot{y}$, and *r* is the desired output (or reference input) for *y*. Our control goal is to drive the output *y* to *r*.

Substituting (3.12) into (3.9) yields

$$u = \frac{k_1(r - z_1) - k_2 z_2 - z_3}{b} \tag{3.13}$$

In (3.13), the controller gains k_1 and k_2 are parameterized in terms of controller bandwidth ω_c. We choose $k_1 = \omega_c^2$ and $k_2 = 2\omega_c$, to place all closed loop poles at -ω_c [7]. The controller represented by (3.13) can drive the output *y* to reference input *r*.

3.3 Stability analysis and external disturbance rejection

Frequency domain analysis is widely used by control engineers for stability and performance analyses. Frequency response provides important information about the behavior of system. It helps to determine system's stability, closed loop bandwidth, and noise attenuation ability. Using frequency response of open loop system to determine the stability of closed loop system is one major advantage of frequency response analysis. Another important advantage of frequency response is that it can be used to design control system. The information about resonant frequencies of a physical system can also be gained from frequency domain analysis.

To perform frequency domain analysis on the torsional plant, the system has to be represented in a transfer function form. In this section, the robustness of ADRC controlled torsional plant against parameter variations, the stability of this control system, and external disturbance rejection capabilities of ADRC will be analyzed.

3.3.1 Transfer function representation of ADRC controlled system

The differential equation modeling of a torsional plant is given by

$$\ddot{\theta} = -a_1\dot{\theta} - a_0\theta + bu \tag{3.15}$$

where,

$$\theta = angular\ position$$

$$u = control\ input$$

$$a_1 = \frac{Friction\ Constant\ (B)}{Inertia\ (J)}$$

$$b = \frac{3 \times K_{SA} \times K_M}{Inertia\ (J)}$$

$$a_0 = 0$$

The generalized disturbance in (3.15) can be represented as $f = -a_1\dot{\theta} - a_0\theta$. The transfer function $G_p(s)$ for the torsional plant in (3.15) can be expressed as (3.16) for which the input of the plant is control effort u, and the output of the system is angular position θ.

$$G_p(s) = \frac{b}{s^2 + a_1 s + a_0} \tag{3.16}$$

Transfer function for ADRC can be expressed as:

$$G_c(s) = \frac{1}{b_0 s} \frac{C_{n2}s^2 + C_{n1}s + C_{n0}}{C_{d2}s^2 + C_{d1}s + C_{d0}} \tag{3.17}$$

Further information about derivation of controller transfer function can be found in frequency response analysis of ADRC [14]. Loop gain transfer function and transfer function from disturbance to output can be better understood from the block diagram given in Figure 6.

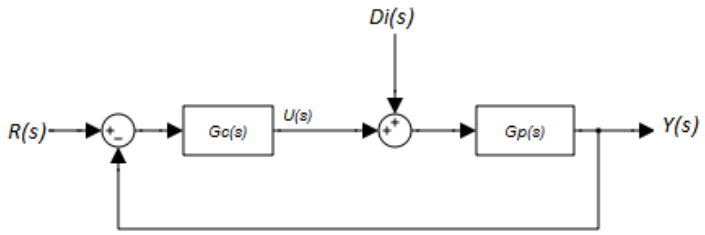

Figure 6: Block diagram of the ADRC controlled torsional system

From Figure 6, loop gain transfer function G_{lg} can be written as

$$G_{lg}(s) = G_p(s)G_c(s) \tag{3.18}$$

To evaluate the performance of ADRC in terms of external disturbance rejection, the transfer function from input disturbance to output can be expressed as:

$$G_{YD}(s) = \frac{G_p(s)}{1 + G_c(s)G_p(s)} \tag{3.19}$$

From (3.18) and (3.19), the stability and external disturbance rejection capability of ADRC will be evaluated in presence of parametric uncertainties.

3.3.2 Stability and robustness analysis

To evaluate the stability of ADRC, the values of four system parameters: inertia J, friction constant B, a_0, and a_1 are changed and the stability margins of control system will be observed. Figure 7 shows the Bode plot of loop gain transfer function in the presence of the variations of inertia J. In this figure, the inertia is varying from -40% to 40% of its nominal value. From the figure, we can see that the frequency response is almost unchanged for different J. Table II shows the stability margins of the loop gain transfer function (3.18) in the presence of the variations of inertia J. From Table II, we can see that the stability margins are positive during the process of varying inertia J from -40% to 40% of its nominal values. Therefore, the control system is robust against the variation of parameter J.

Figure 8 shows the Bode diagrams of the loop gain transfer function as the friction constant B is changing from -90% of to 100 times its nominal value. Table III shows the stability margins of the loop gain transfer function as the friction constant B is changing from -90% of to 100 times its nominal value. Again, from the figure and table, we can see that the stability margins are positive and are almost unchanged with the change of friction constant. The ADRC controlled torsional system shows excellent robustness and stability features against system uncertainties.

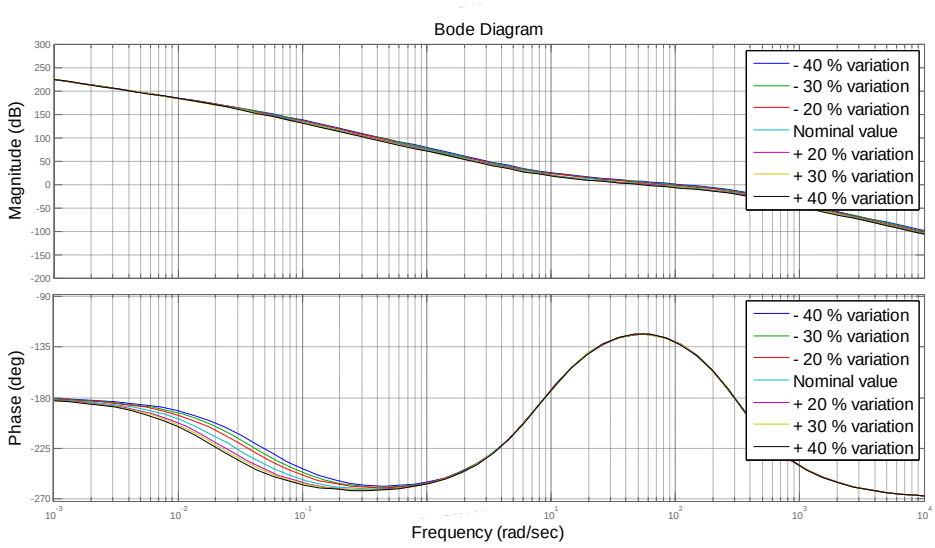

Figure 7: Frequency response of loop gain transfer function with the change of inertia *J*

TABLE II: STABILITY MARGINS WITH THE CHANGE OF INERTIA J

Parameter Values of Inertia (*J*)	**Gain Margin (db)**	**Phase Margin (*degrees*)**
-40 %	4.4228	48.5739
-30 %	5.1597	51.5090
-20 %	5.8967	53.4862
Nominal value J	7.3705	55.6005
+20 %	8.8444	56.2260
+30 %	9.5813	56.1910
+40%	0.1067	55.9918

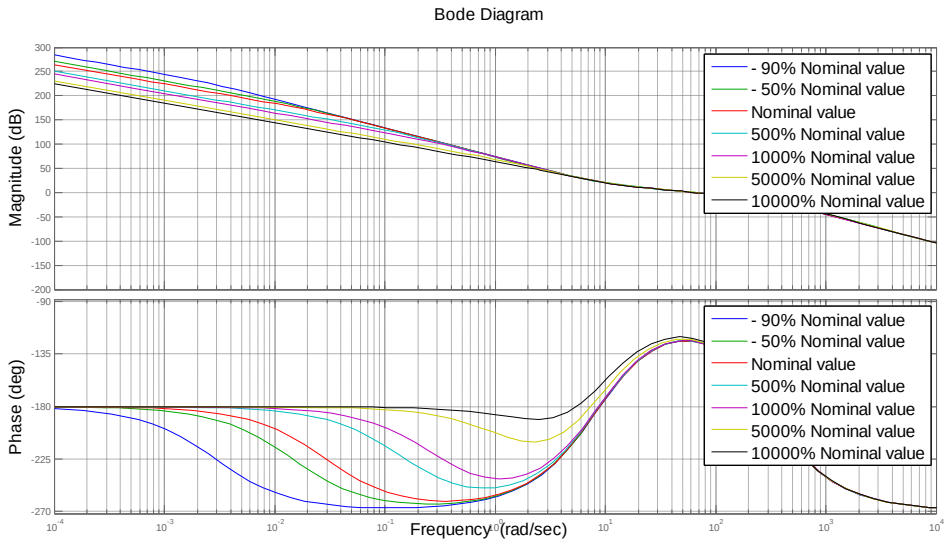

Figure 8: Frequency response with the change of friction constant *B*

TABLE III: STABILITY MARGINS WITH THE CHANGE OF FRICTION CONSTANT

Parameter Values of Friction (*B*)	**Gain Margin (db)**	**Phase Margin (*degrees*)**
-90 %	7.3694	55.5778
-50 %	7.3699	55.5879
Nominal value	7.3705	55.6005
500 %	7.3755	55.7016
1000 %	7.3816	55.8280
5000 %	7.4312	56.8405
10000 %	7.4934	58.1093

Figure 9 shows the Bode diagrams of loop gain transfer function as a_1 is changing from -90 of to 100 times its nominal value. Table IV shows the stability margins as a_1 is changing from -90 of to 100 times its nominal value. From the table, we can see the stability margins are almost unchanged with the change of a_1.

Figure 10 shows the Bode diagrams of the loop gain transfer function as the parameter a_0 changes from 0.1 to 100. Nominal value of a_0 is zero. Table V lists the stability margins of the loop gain transfer function as the parameter a_0 is changing from 0.1 to 100. The frequency response and stability margins show the stability and robustness of the ADRC against the variations of parameter a_0.

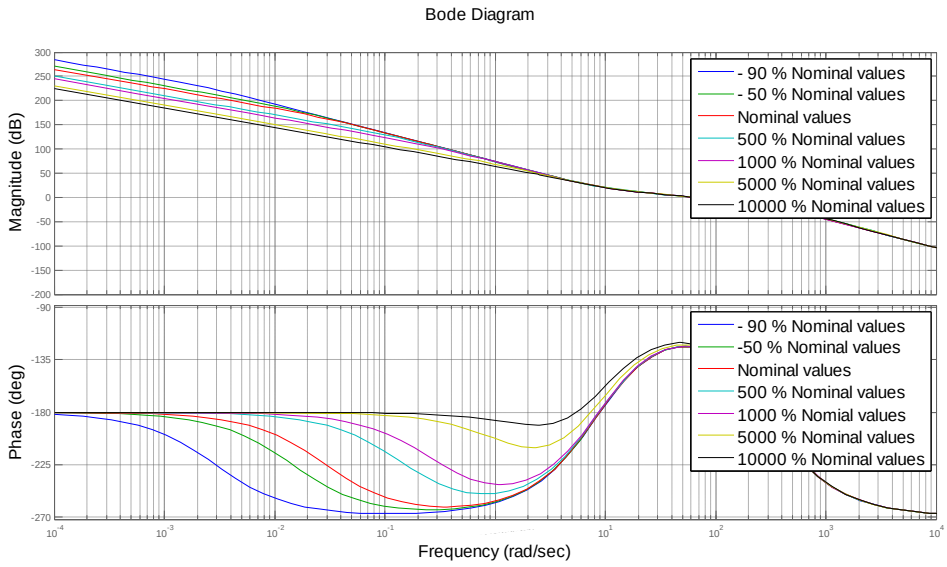

Figure 9: Frequency response with the change of a_1

TABLE IV: STABILITY MARGINS WITH PARAMETER VARIATIONS

Parameter values of a_1	**Gain Margin (db)**	**Phase margin (*degrees*)**
-90 %	7.3694	55.5778
-50 %	7.3699	55.5879
Nominal value	7.4312	55.6005
500 %	7.4312	55.7016
1000 %	7.4312	55.8280
5000 %	7.4312	56.8405
10000 %	7.4934	58.1093

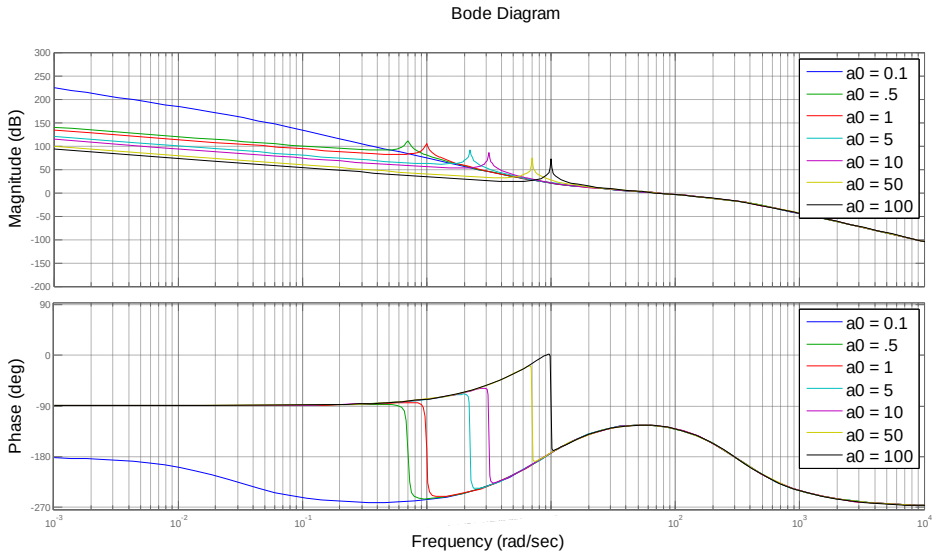

Figure 10: Frequency response with the change of a_0

TABLE V:STABILITY MARGINS WITH CHANGE IN PARAMETER VALUES

Parameter values of a_0	**Gain Margin (db)**	**Phase margin (*degrees*)**
0	7.3705	55.6005
0.5	7.3705	55.5999
1	7.3704	55.5992
5	7.3701	55.5936
10	7.3697	55.5865
50	7.3663	55.5272
100	7.3625	55.4527

Figure 11 shows the frequency response of loop gain transfer function in the presences of the parameter variations for both a_0 and a_1. Table VI lists the stability margins of the system in the presences of the parameter variations for both a_0 and a_1. Figure 11 and Table VI demonstrate the stability and robustness of the ADRC controlled torsional plant against the variations for both a_0 and a_1.

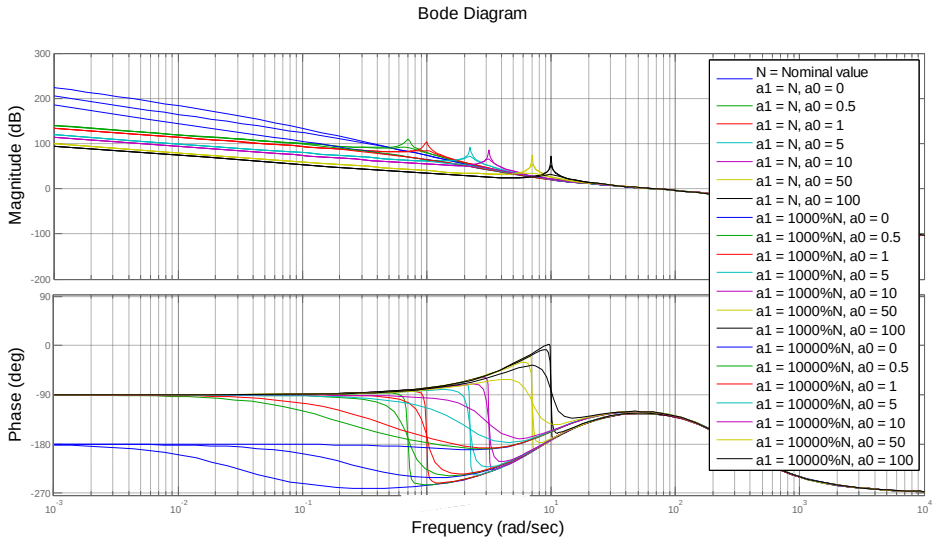

Figure 11: Frequency response for the changes of a_1 and a_0

TABLE VI: STABILITY MARGINS WITH THE CHANGES OF PARAMETER VALUES

Parameter values of a_0 for $a_1 = 1$	**Gain Margin (db)**	**Phase margin (*degrees*)**
0	7.3705	55.6005
0.5	7.3705	55.5999
1	7.3704	55.5992
5	7.3701	55.5936
10	7.3697	55.5865
50	7.3663	55.5272
100	7.3625	55.4527
Parameter values of a_0 for $a_1 = 10$	**Gain Margin (db)**	**Phase margin (*degrees*)**
0	7.3816	55.8280
0.5	7.3816	55.8274
1	7.3816	55.8267
5	7.3812	55.8211
10	7.3808	55.8141
50	7.3775	55.7549
100	7.3736	55.6805
Parameter values of a_0 for $a_1 = 100$	**Gain Margin (db)**	**Phase margin (*degrees*)**
0	7.4934	58.1093
0.5	7.4934	58.1086
1	7.4933	58.1079
5	7.4930	58.1026
10	7.4926	58.0958
50	7.4893	58.0381
100	7.4854	57.9

Figures 7, 8, 9, 10 and 11 demonstrate stability and robustness of ADRC in presence of system uncertainties.

3.3.3 External disturbance rejection

In this section, the frequency response for the transfer function from input disturbance to output position given by (3.19) is demonstrated in order to evaluate the external disturbance rejection capability of ADRC. In addition, the system parameters are varied to examine the effects of parametric uncertainties on disturbance rejection capability of the controller. Figures 12, 13 and 14 demonstrate effectiveness of ADRC in rejecting external disturbance in presence of plant parametric uncertainties. In Figure 12 and Figure 13, parameters are varied individually whereas in Figure 14 parameters are varied simultaneously.

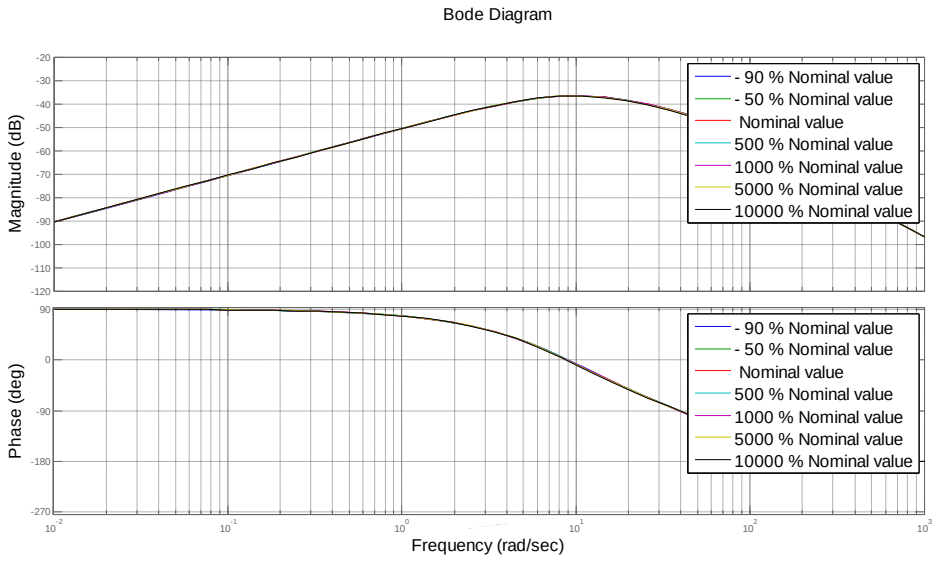

Figure 12: External disturbance rejection in the presence of the change of a1

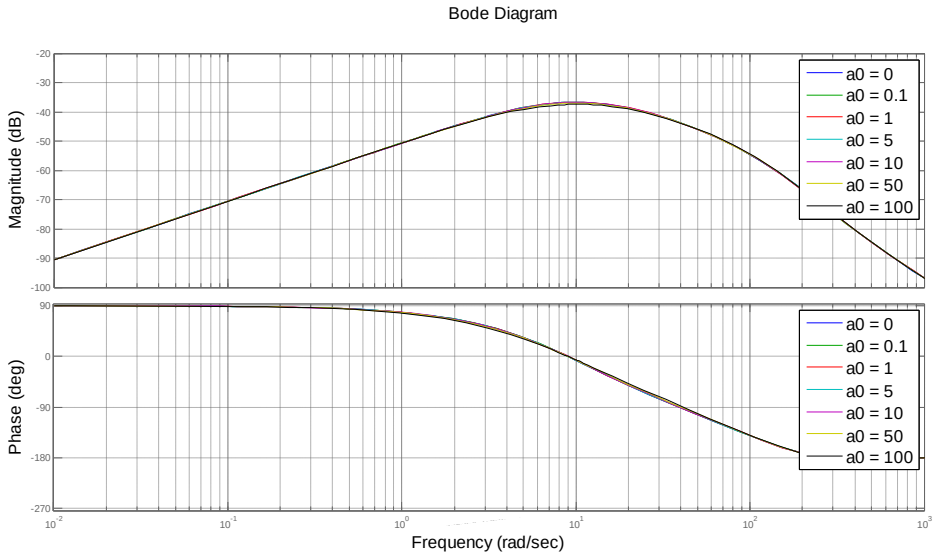

Figure 13: External disturbance rejection in the presence of the change of a_0

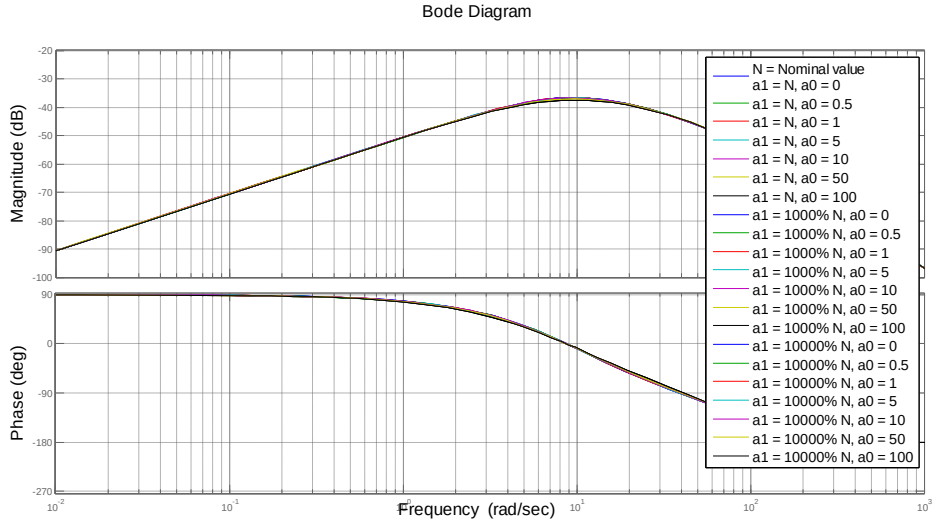

Figure 14: External disturbance rejection in the presences of the changes of a_0 and a_1

3.4 Summary of the chapter

In this chapter, design of ADRC controller is discussed. Design of ADRC is divided in two parts, extended state observer is used to estimate internal states of plant along with disturbance and PD controller to control second order integral plant. After controller design, stability analysis and external disturbance rejection is discussed. In next chapter, simulation of ADRC on mathematical model of torsional plant is discussed.

CHAPTER IV

CONTROLLER SIMULATION

4.1 ADRC simulation on torsional plant model

In this chapter, the simulation of ADRC will be conducted on the mathematical model of torsional plant. The ADRC controller including ESO (given by (3.7), (3.8), and (3.13)) is applied to the torsional plant represented by (3.5) and (3.6). The system inertia is J = 0.004312 and friction constant B = 0.00078. The Simulink model about the implementation of the ADRC on the torsional plant is shown in Appendix B. Figures 15, 16, and 17 show the simulation results on a mathematical model of the torsional plant as the reference input is motion profile. The output response of the mathematical model of the torsional plant is shown in Figure 15. From this figure, we can see that the ADRC successfully drives the position output of the plant to reference signal in the presences of disturbance.

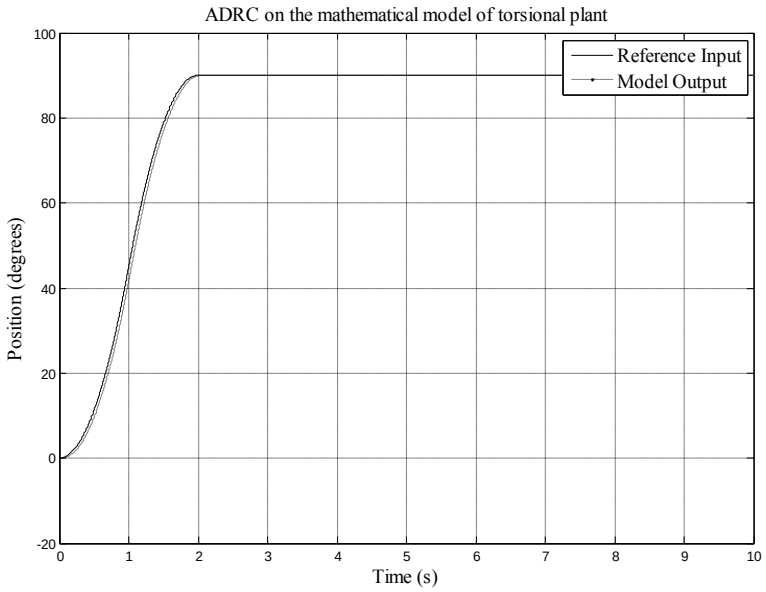

Figure 15: The output response of ADRC controlled torsional plant model as the reference signal is a motion profile

The control effort of ADRC is shown in Figure 16.

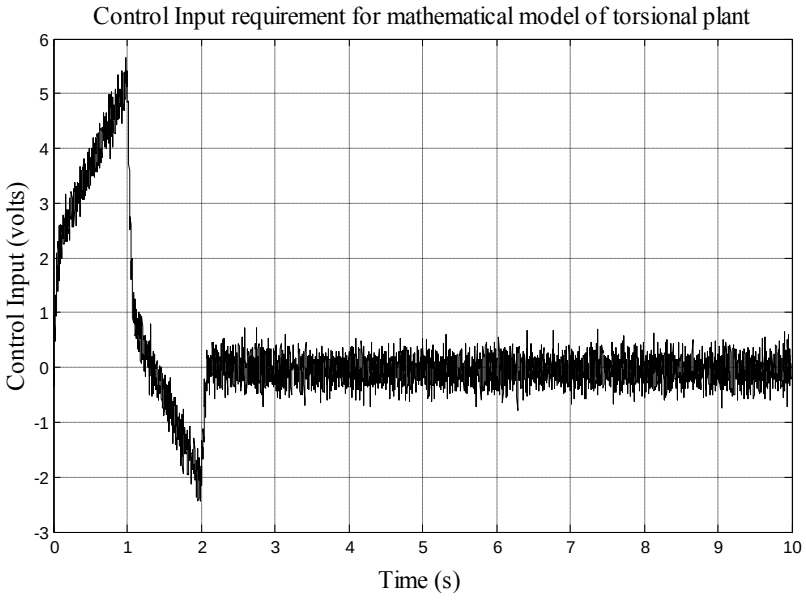

Figure 16: Control input for the mathematical model of the torsional plant as input is motion profile

The performance of extended state observer is shown in Figure 17 where the estimates of position, velocity and disturbance are given along with tracking error for

position. Good performance of extended state observer is essential in order to obtain desired performance with ADRC controller. Figure 17 shows the excellent estimations of position, velocity, and generalized disturbance using extended state observer.

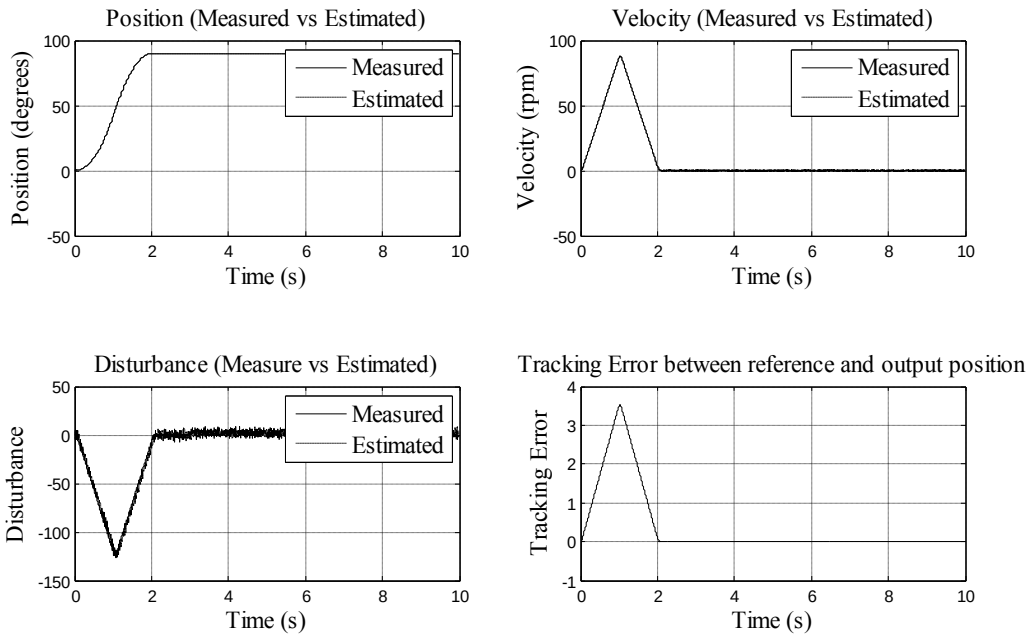

Figure 17: Estimated position, velocity, and generalized disturbance and position tracking error as input is motion profile

Figure 18 shows the output response of the mathematical model of torsional plant when the reference input is a step input.

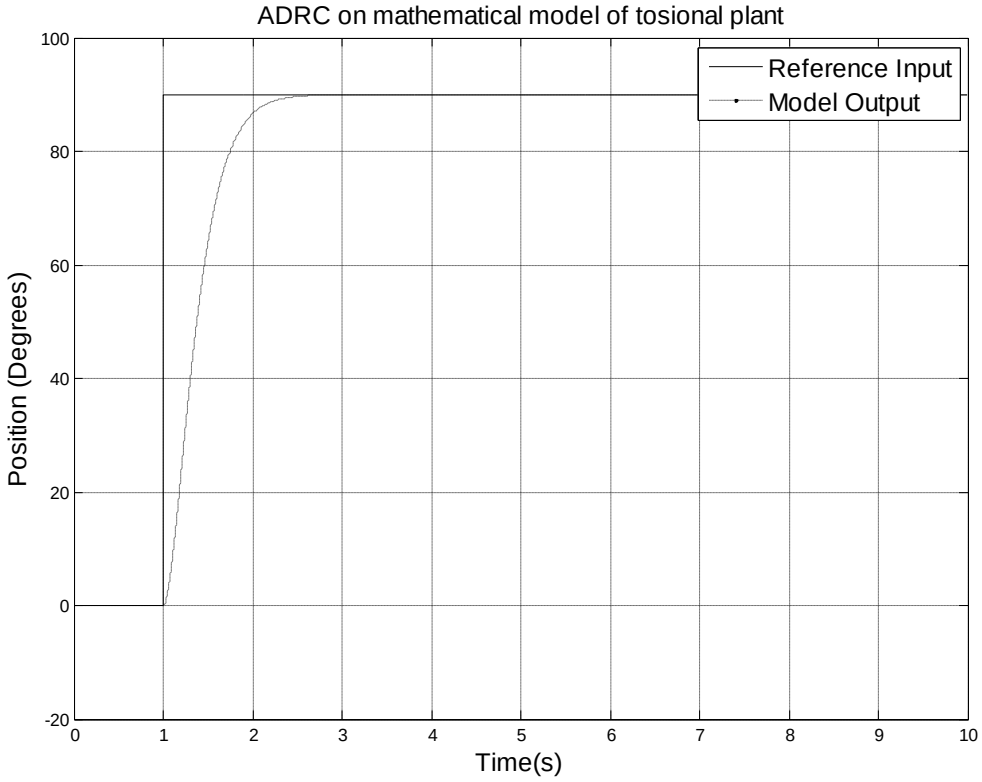

Figure 18: The output response of ADRC controlled plant with step reference input

From Figure 18, we can see that ADRC controller achieves good performance with step input. Figure 19 shows control effort required to produce desired output response for step input.

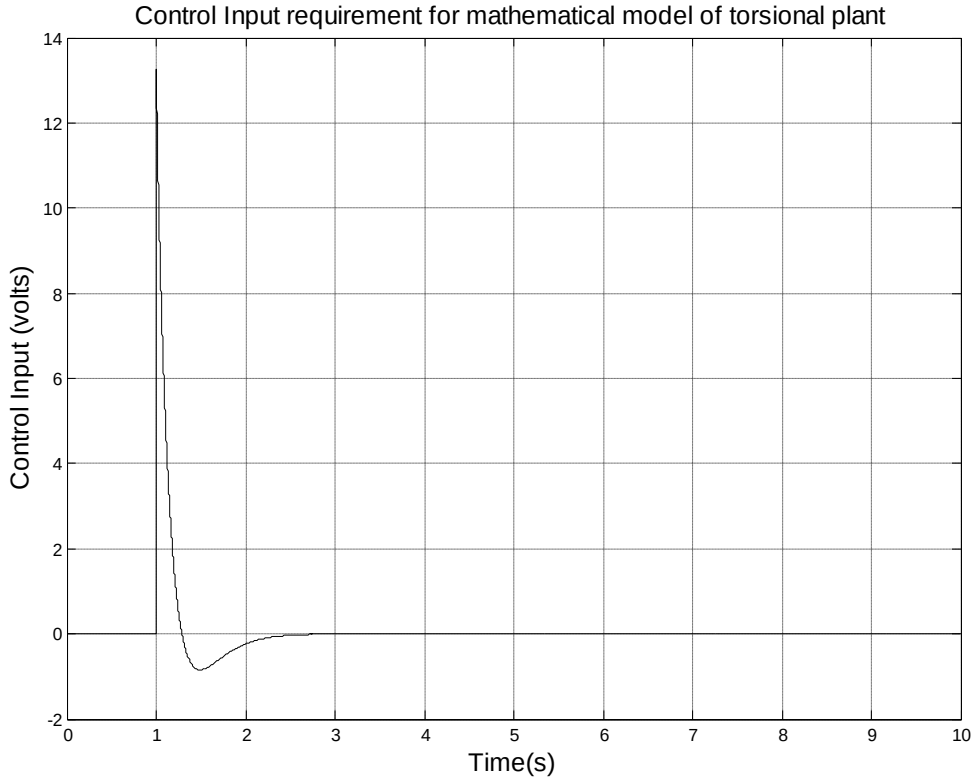

Figure 19: Control effort as the reference signal is a step input

As mentioned before, the performance of ADRC is greatly dependent on the performance of ESO. In Figure 20, the estimation performance of ESO in tracking position output, angular velocity and disturbance is shown with step input. From the figure, we can see excellent performance of extended state observer in estimation of position, velocity and disturbance. The figure also demonstrates the good position tracking performance of ADRC.

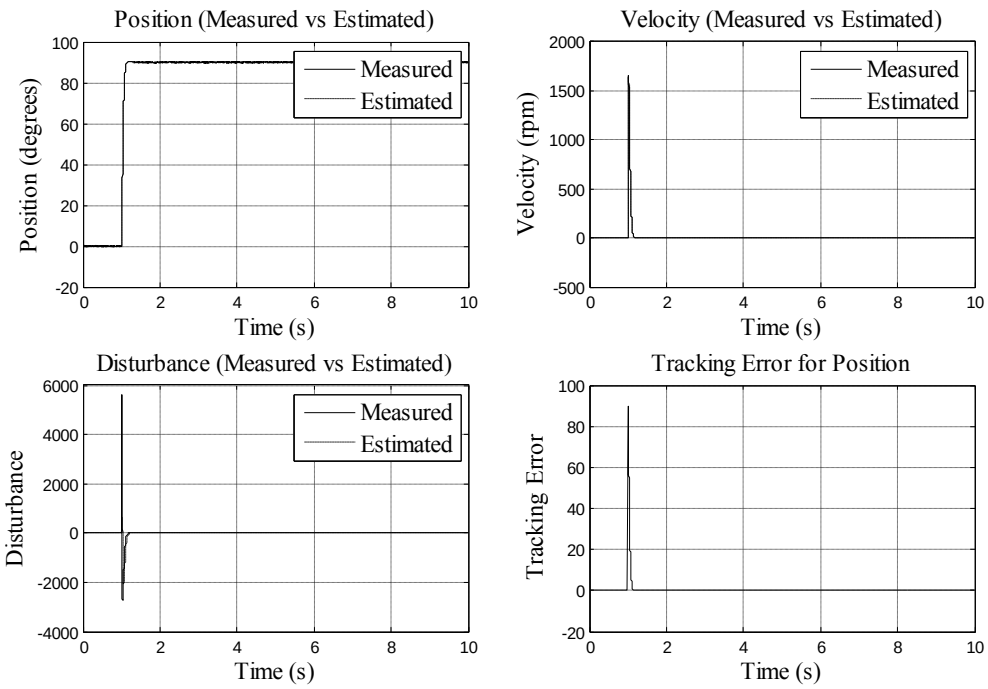

Figure 20: Estimated position, velocity, and disturbance and tracking error

4.2 Summary of the chapter

Simulation of ADRC controller on mathematical model of torsional plant is discussed in this chapter. Simulation proves that effectiveness of ADRC controller in achieving position control for a motion profile input and a step input as reference. Implementation of ADRC on actual torsional plant is discussed in next chapter.

CHAPTER V

HARDWARE IMPLEMENTATION

5.1 Implementation of ADRC on torsional plant

In this chapter, the performance of the ADRC controller will be examined on a real torsional plant with the uses of Matlab Real-time workshop and Real-time windows target. A set of I/O blocks are available in Real-time windows target that are used to create an interface between Simulink model and real torsional plant. I/O blocks connect with the torsional plant through multifunction I/O card and read plate position from encoder card. PCI-DAS 1002 analog and digital I/O board is used to provide control voltage to dc servo motor and PCI-QUAD04 encoder card is used to read plate position. Resolution of encoder is 16000 lines per revolution of the plate.

A simulation model is created that consists of controller, extended state observer and I/O blocks. I/O blocks in Simulink are used to apply control signal to actual torsional plant and to read output position of the rotating plate.

The effects of parameter variations, friction and external disturbance, actuator constraints, sensor dynamics and measurement noise on the controller will be studied in this chapter. Implementing the ADRC on real system shows the feasibility and practicality of the controller design in reality.

In the rest part of the section, the system responses for two different types of inputs: step input and a motion profile will be shown. The capability of ADRC to handle external disturbance will also be investigated. Both ADRC and PD controller will be applied to and implemented on the torsional plant. The controller features such as ease of tuning, tracking performance and control voltage requirements for both types of controllers will be discussed.

Figure 21 shows output response of an ADRC controlled torsional plant for a motion profile input. External disturbance is applied at 6.6 seconds. It demonstrates the effectiveness of ADRC in rejecting the external disturbance which is applied to the system at 6.6 seconds. From Figure 21, it can also be seen that ADRC achieves excellent tracking performance for a motion profile even in the presence of disturbance.

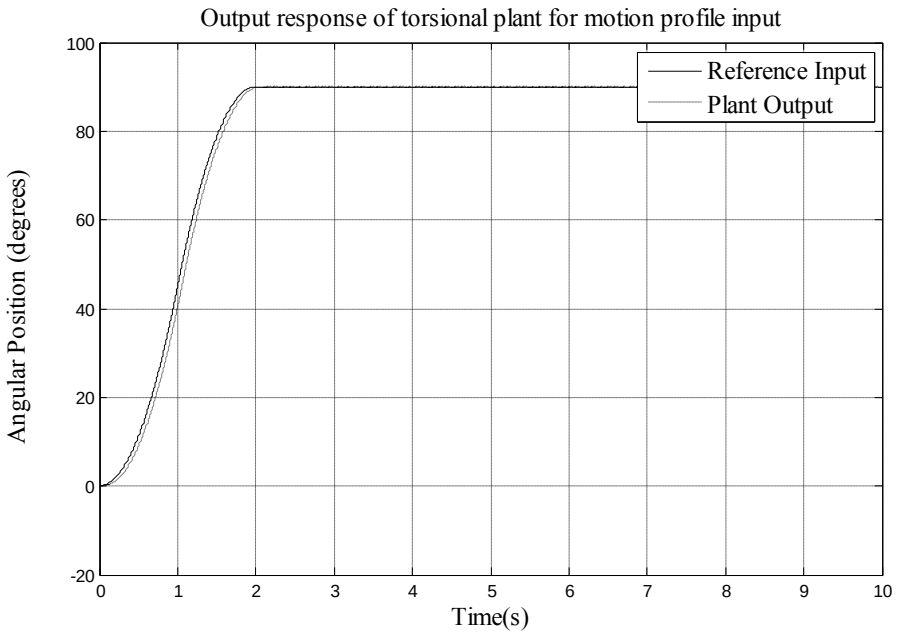

Figure 21: Output response of torsional plant for a motion profile reference

The required control input for the output response in Figure 21 is given in Figure 22.

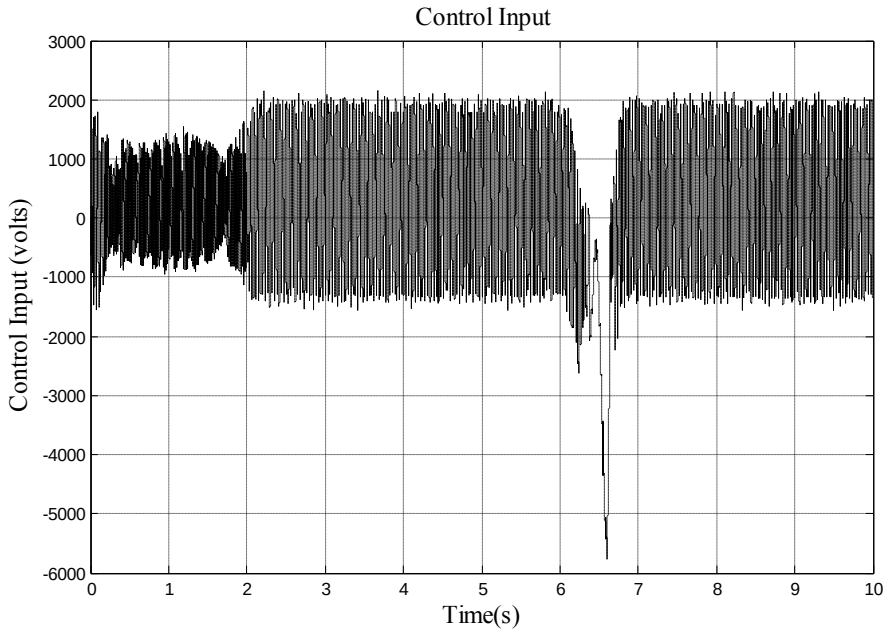

Figure 22: The output of ADRC controlled plant with motion profile as reference input

Besides motion profile, step input is also very widely used in experimental control design. So the output response to a step input will be evaluated in the following part. In Figure 23, the output response of a torsional plant to a step input is given.

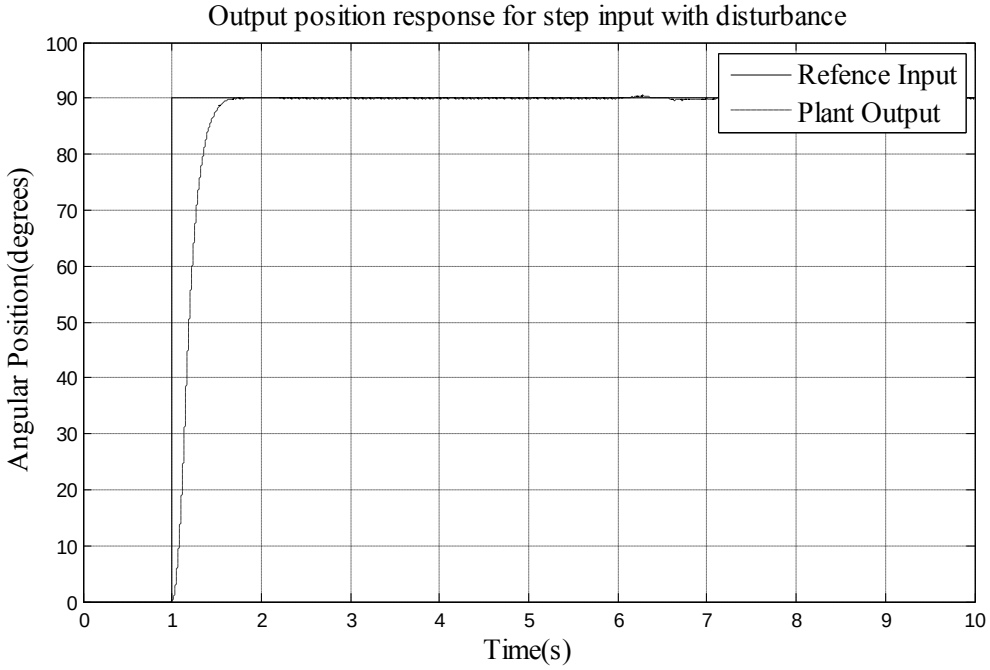

Figure 23: Output response of ADRC controlled torsional plant with a step reference input

It can be seen in Figure 23 that for step input, ADRC obtains very good tracking performance even in the presence of external disturbance. Figure 24 shows the tracking error of position with step input as reference input. The plate changes position from 0 degree to 90 degree at t =1 second. This is why there is a big spike in tracking error at t=1 second. The control effort for step input is shown in Figure 25.

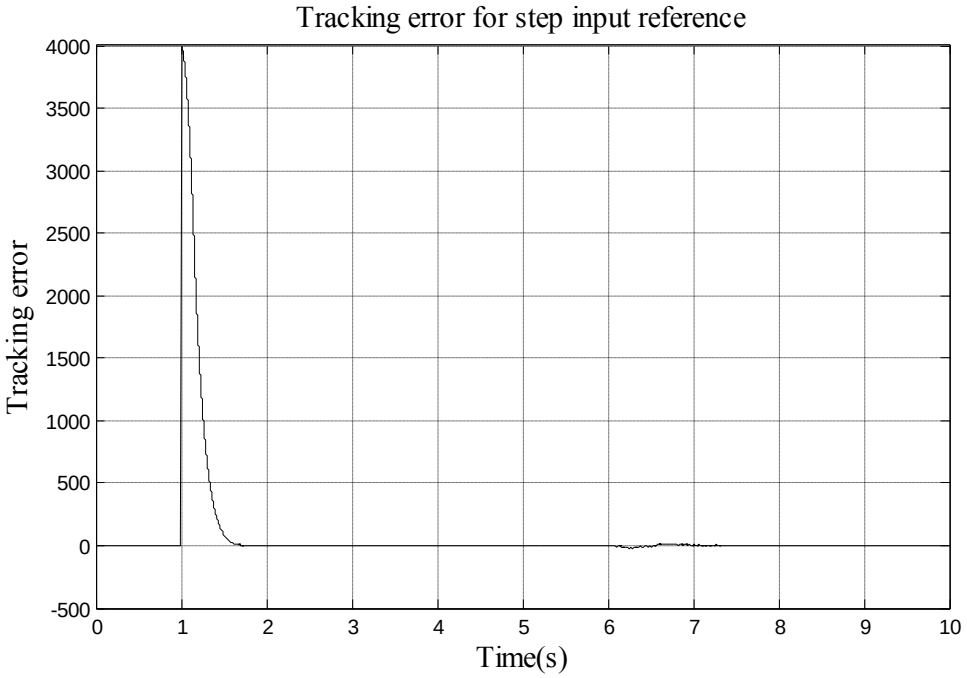

Figure 24: Tracking error of position in the presence of external disturbance as step input is reference input

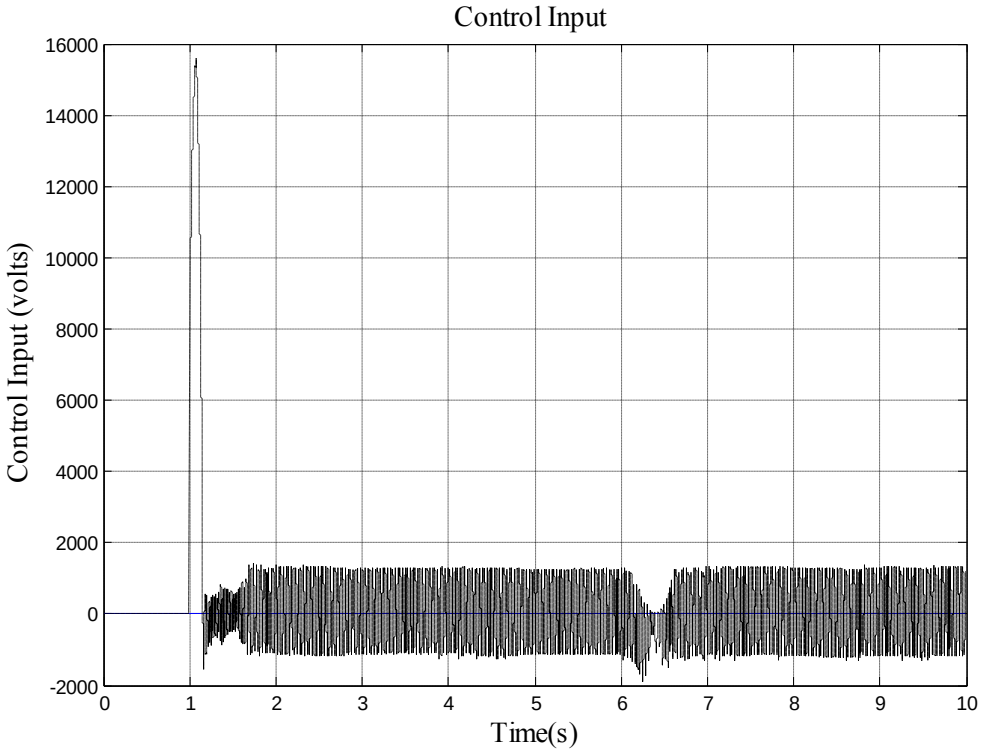

Figure 25: The output of ADRC controller with step reference input

In Figure 25, there is a big spike value for the control effort at the initial part. It is not feasible to provide such a spike value in practice. Therefore, we make the control input bounded within a range of -0.8 V to +0.8 V. Then we will obtain the control effort shown in Figure 26. For hardware implementation purpose, only bounded input is used in this study. A bounded input within range of -0.8 V to +0.8 V results in excellent tracking performance by ADRC controlled torsional plant for motion profile and step as a reference input.

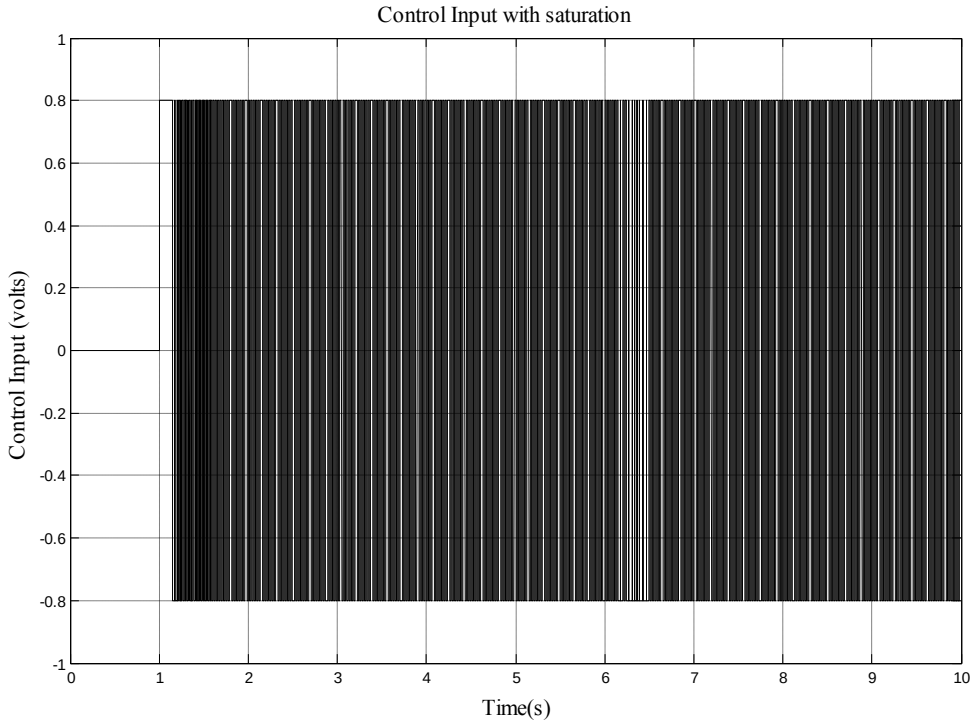

Figure 26: Bounded control input

A closed-up view of the bounded control effort is shown in Figure 27.

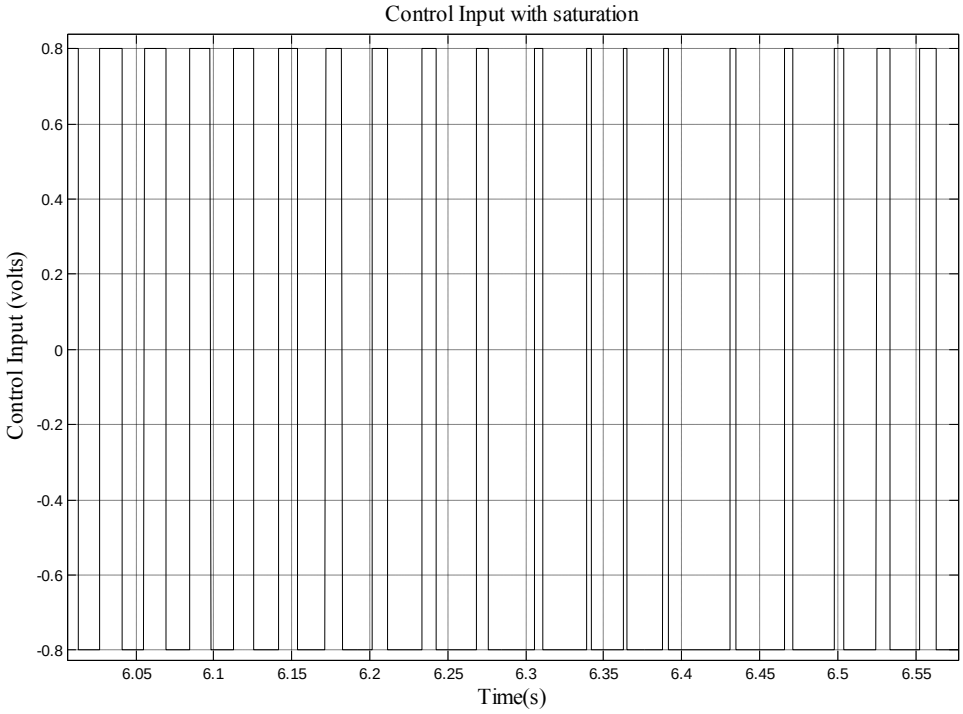

Figure 27: Control Input in a small time interval

Figures 21 through 27 show the simulation results with two different types of reference inputs.

Next, the results of ADRC will be compared with that of PD controller, which is still the most popular controller in industrial control applications. Output response of the torsional plant under the control of a PD controller will be given.

5.2 Implementation of PD controller on torsional plant

The Simulink model about the implementation of a PD controller on the torsional plant is given in Appendix D. Figure 28 shows the block diagram for the implementation of PD controller on torsional plant.

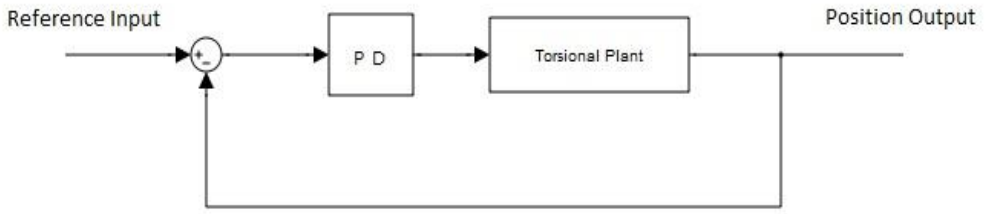

Figure 28: Block diagram for implementation of PD controller on torsional plant

The formula of PD controller is given as follows.

$$u(t) = k_p e(t) + k_d \frac{d}{dt} e(t) \tag{5.1}$$

For hardware implementation of PD controller, the controller parameters are k_p = 1.365, and k_d = .637. In Figure 28, the angular position of the rotational plate of torsional plant is controlled by PD controller. Step input and motion profile are used as reference inputs for the PD controlled plant. Our control objective is to make the angular position output track the reference input in the presences of disturbance and parameter variations.

Figure 29 shows output response of torsional plant for a PD controller. Motion profile is used as a reference input. It can be seen that good tracking performance is obtained with PD controller.

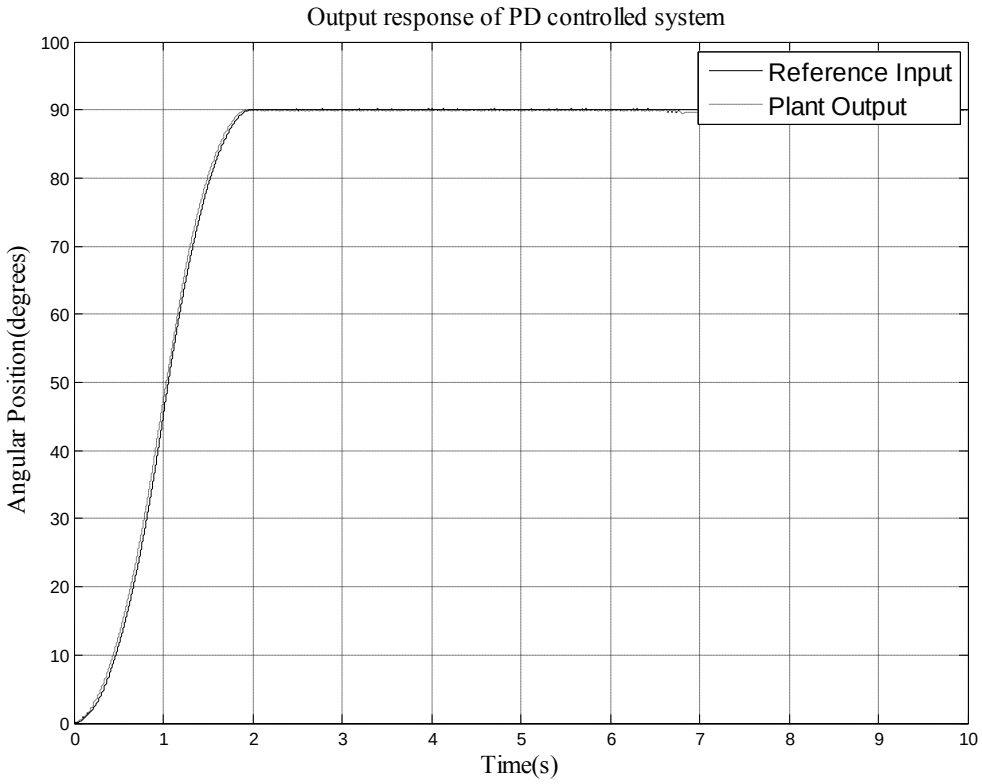

Figure 29: The output response of PD controlled plant with motion profile as reference signal

Figure 30 shows the output response of PD controlled plant with step input as reference input. It can be seen that good tracking performance is obtained with PD controller.

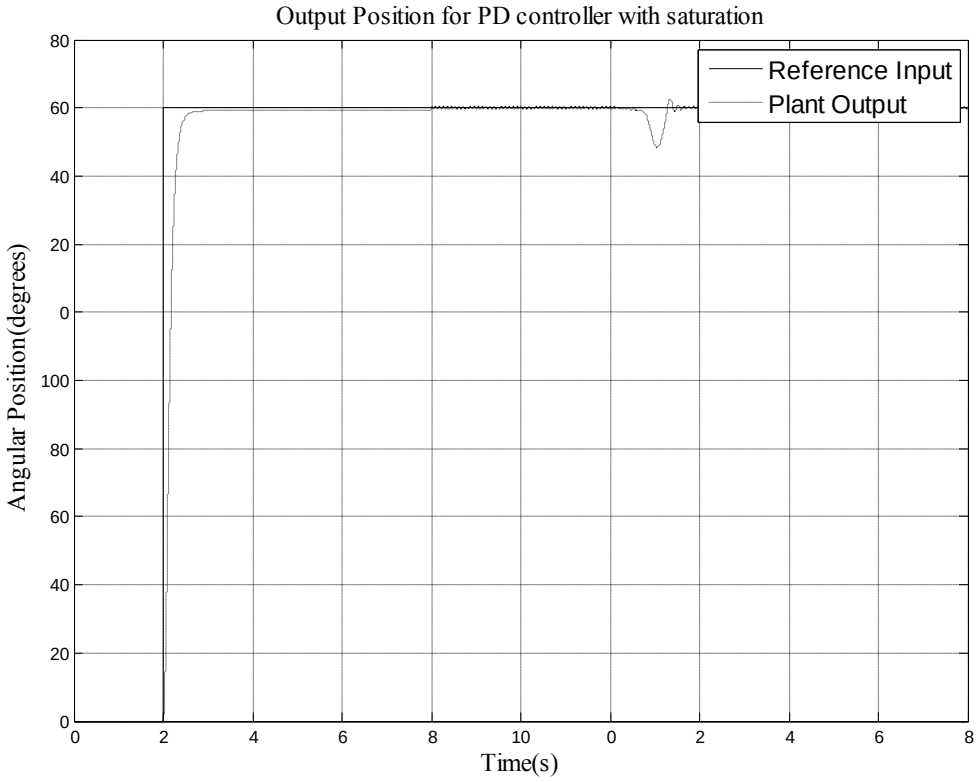

Figure 30: The output response of PD controlled plant with step reference signal

Figure 31 shows the PD control effort when step input is a reference signal. In Figure 31, a very high initial voltage spike can be observed at t=1s. It is not possible to provide such high value. A saturated control input has to be used. However, it will result in performance deterioration.

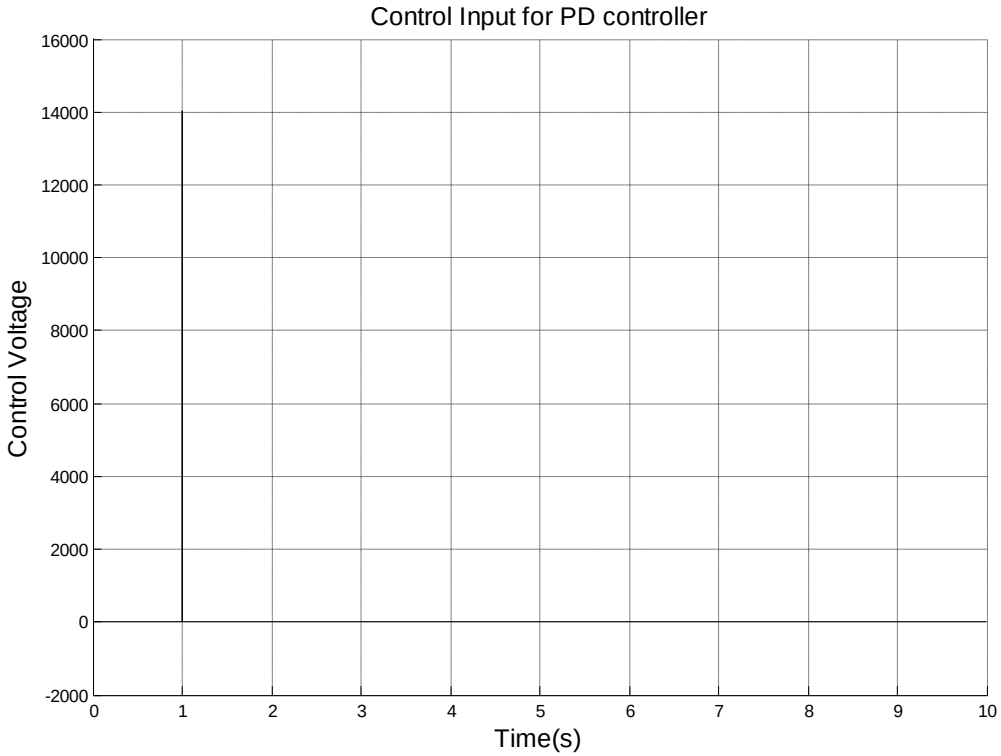

Figure 31: Control Input for PD controller

5.3 Performance comparison between ADRC and PD controller

Figure 32 shows the output responses for ADRC and PD controlled systems when motion profile is used as a reference input signal. From the figure, we can see that both ADRC and PD controlled plants show excellent tracking performances.

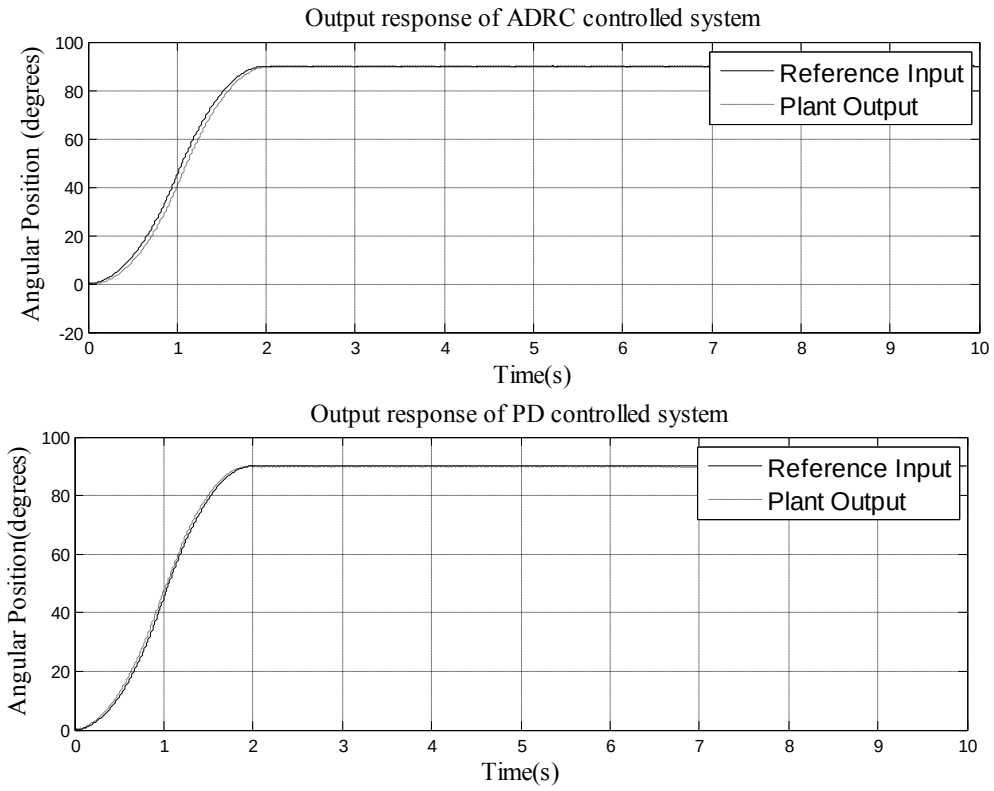

Figure 32: Output of ADRC and PD controlled plants as the reference input is motion profile

Figure 33 and Figure 34 shows the performance comparison between ADRC and PD controller for step reference input. Improved performance of ADRC can be clearly seen in the figure. External disturbance rejection of ADRC is better as compared to that of a PD controller.

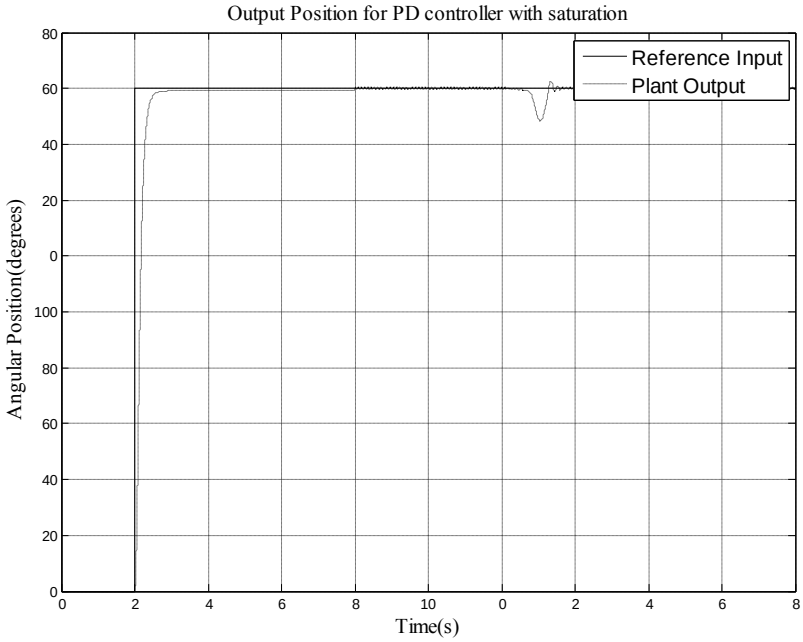

Figure 33: Output response of PD controlled plant with step input as reference and external disturbance at t=6s

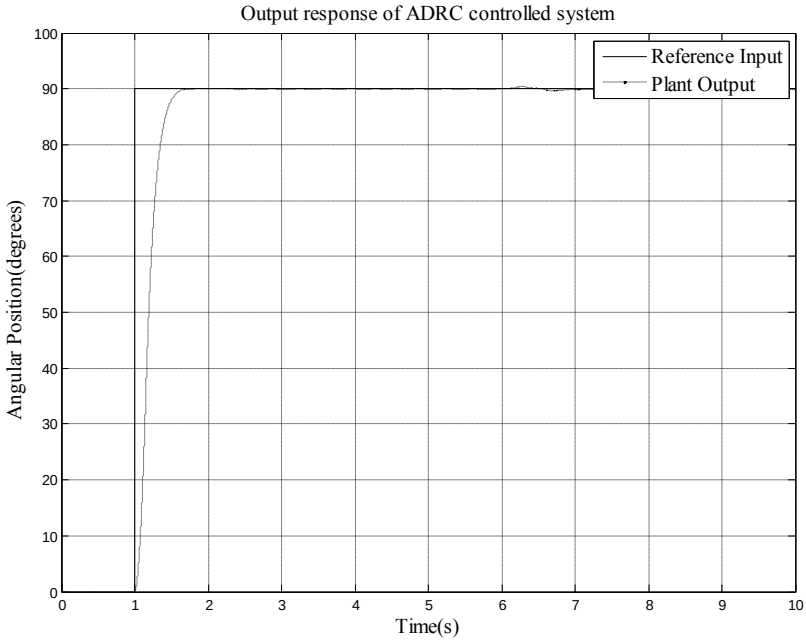

Figure 34: Output response of ADRC controller plant with reference input as step input with external disturbance at t=6s

5.4 Summary of the chapter

In this chapter, hardware implementation of ADRC is discussed. Output response of ADRC and PD controllers are compared. ADRC controller provides superior tracking performance and compared to PD controller. ADRC controller is simple to implement and easy to tune with parameterization of observer and controller gains.

CHAPTER VI

CONCLUDING REMARKS AND FUTURE WORK

6.1 Concluding Remarks

The design and implementation of ADRC on torsional plant have been developed in this thesis. The dynamic modeling of the torsional plant was introduced as well. The effectiveness of ADRC is first verified on a mathematical model and then on the actual torsional plant. Both simulation and implementation results demonstrate the effectiveness of the ADRC. In addition, frequency-domain analyses were conducted on the ADRC controlled torsional plant. The analyses proved the stability and robustness of the ADRC against external disturbance and parameter variations. The performance of ADRC is compared to that of PD controller since the PD controller is the most widely used controller in industry. The comparison study shows that the ADRC is more effective in achieving the control objective and is simpler to implement and easier to tune than PD controller.

6.2 Future Work

Implementation of ADRC is highly dependent on proper tuning of observer and controller bandwidths. Proper selection of controller and observer bandwidths greatly depends on sensor and actuators used in the torsional plant to be controlled. If controller bandwidth is too large, it will be not feasible to implement it in practice and the control performance will be degraded. If observer bandwidth is too big, noise in measurement will affect the control system's performance. So fine tuning of controller and observer bandwidths will be continued to study in the future. For implementing ADRC, the knowledge about controller gain and the relative order of system are required to be known. To what degree of success ADRC can be implemented without the knowledge of these parameters would be an interesting option to explore in the future as well.

In addition, since the torsional plant studied in this thesis resembles to a class of rotational systems, the ADRC that is successfully implemented on it can be extended for use in other similar systems with minor modifications in the future.

REFERENCES

[1]. Z. Gao and R. Rhinehart, "Theory vs. Practice: The Challenges from Industry," in *Proc. of American Control Conference*, pp. 1341-1349, Boston, Massachusetts, June 30-July 2, 2004.

[2]. F.L. Lewis, Applied Optimal Control and Estimation, Prentice Hall, 1992.

[3]. N. Minorsky, "Directional Stability and Automatically Steered Bodies," *Journal of the American Society of Naval Engineer*, vol. 34, p. 280, 1922.

[4]. W.S. Levine, the Control Handbook, CRC Press and IEEE Pres, 1996.

[5]. H.Lee and M. Tomizuka, "Robust motion controller design for high-accuracy positioning systems," *IEEE Transactions on Industrial Electronics*, vol. 43, pp. 48-55, 1996.

[6]. Q Zheng, "On active disturbance rejection control: stability analysis and application in disturbance decoupling control*,"* PhD Dissertation, Cleveland State University, 2009.

[7]. Z. Gao, Y. Huang, and J. Han, "An Alternative Paradigm for Control System Design," in *Proc. of IEEE conference on Decision and Control*, vol. 5, Page(s):4578 – 4585, 4-7 Dec. 2001.

[8]. A. Radke and Z. Gao, "A survey of state and disturbance observers for practitioners," in *Proc. of the 2006 American Control Conference*, pp. 5183-5188, Minneapolis, Minnesota, USA, Jun 14-16, 2006.

[9]. S. Kwon and W. K. Chung, "*A* discrete-time design and analysis of perturbation observer for motion control applications," *IEEE Transactions on Control Systems Technology*, vol. 11, no. 3, pp. 399-407, 2003.

[10]. J. Han, "A class of extended state observers for uncertain systems," *Control and Decision*, vol. 10, no. 1, pp. 85-88, 1995. (In Chinese)

[11]. J. Han, "Auto-disturbance rejection control and its applications," *Control and Decision*, vol. 13, no. 1, pp. 19-23, 1998. (In Chinese)

[12]. Z. Gao, "Scaling and Bandwidth-Parameterization Based Controller Tuning," in *Proc. of American Control Conference*, pp.4989-4996, Denver, Colorado, USA, June 2003.

[13]. R. Miklosovic, A. Radke, and Z. Gao, "Discrete Implementation and Generalization of the Extended State Observer," in *Proc. of American Control Conference*, pp. 2209-2214,Minneapolis, Minnesota, USA, June 14-16, 2006.

[14]. L. Dong, D. Avanesian, "Drive-mode Control for Vibrational MEMS Gyroscopes", *IEEE Transactions on Industrial Electronics*, vol. 56, no. 4, pp. 956¬963, Apr. 2009.

[15]. G. Tian and Z. Gao, "Frequency Response Analysis of Active Disturbance Rejection Based Control System", in *Proc. of IEEE International Conference on Control Application*, Singapore, pp. 1595-1599, Oct. 2007.

[16]. One Degree of Freedom Torsional plant system: Positioning and Speed Control, The University of Texas - Pan American, Department of Mechanical Engineering, Edinburg, Texas 79541-2999 [Online]. Available:http://www.engr.panam.edu/~kypuros/CCLI/TorsionPlant/TorsionPlantWOSpringControl1 DOF.html

[17]. *Torsional Control System, Manual for Model* M205*a*, Educational Control Products, Bell Canyon, California.

[18]. Verification and validation of models, Michigan State University, Department of Computer Science and Engineering, East Lansing, Michigan, 48825-1302. [Online].
Available: www.cse.msu.edu/~cse808/note/lecture11.ppt

[19]. Z. Gao "Active Disturbance Rejection Control: A Paradigm Shift in Feedback Control Design," in *Proc. of American Control Conference*, pp. 2399-2405, Minneapolis, Minnesota, USA, Jun. 14-16, 2006.

[20]. J. Han, "Nonlinear state error feedback control, " *Control and Decision*, vol. 10, no. 3, pp. 221-225, 1995. (In Chinese)

[21]. Z. Gao, S. Hu, and F. Jiang, "A Novel Motion Control Design Approach Based On Active Disturbance Rejection," in *Proc. of IEEE Conference on Decision and Control*, Orlando, vol.5, pp 4877-4882, December 4-7, 2001.

[22]. Q. Zheng and Z. Gao, "Motion Control Optimization: Problem and Solutions," *International Journal of Intelligent Control and Systems*, vol. 10, no. 4, pp. 269-276, 2006.

[23]. F. Goforth, "On Motion Control Design and Tuning Techniques," in *Proc. of the 2004 American Control Conference*, Boston, Massachusetts, USA pp. 716-721, June 30 - July 2, 2004.

[24]. Q. Zheng and Z. Gao, "Active Disturbance Rejection Control for Chemical Processes," in *Proc. of the IEEE Conference on Control Applications*, pp 855-861, Singapore, Oct. 1-3, 2007.

[25]. Y. Hou, Z. Gao, F. Jiang, and B. Boulter, "Active disturbance rejection control for web tension regulation," in *Proc. of the 40th IEEE Conference on Decision and Control*, vol. 5, pp. 4974-4979, Orlando, Florida, USA, Dec. 4-7, 2001.

[26]. Y. Zhang, "Load Frequency Control of Multiple-Area Power Systems", Master's Thesis, Cleveland State University, 2009.

[27]. Q. Zheng, L. Dong, D. H. Lee, and Z. Gao, "Active Disturbance Rejection Control for MEMS Gyroscopes," in *Proc. of the American Control Conference*, pp. 4425-4430, Seattle, Washington, USA, June 11-13, 2008.

[28]. L. Dong, Q. Zheng and Z. Gao, "On Control System Design for the Conventional Mode of Operation of Vibrational Gyroscopes," *IEEE Sensors Journal*, vol. 8, no. 11, pp. 1871-1878, 2008.

[29]. R. Miklosovic and Z. Gao, "A Dynamic Decoupling Method for Controlling High Performance Turbofan Engine," in *Proc. of the 16th IFAC World Congress*, Prague, Czech Republic, July 4-8, 2005.

APPENDICES

APPENDIX A: Simulink setup for model validation

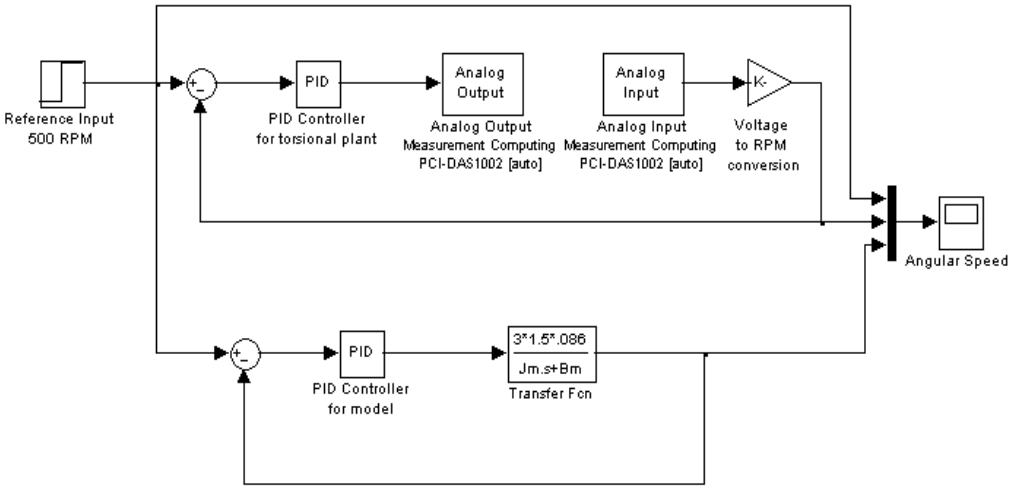

APPENDIX B: Simulink setup for implementation of ADRC on torsional plant

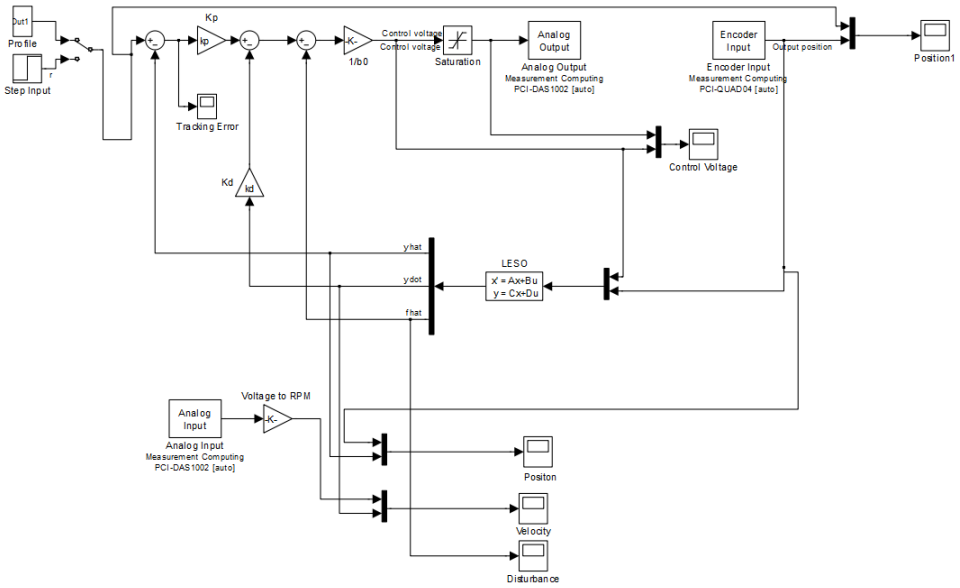

APPENDIX C: Simulink setup for implementing PD controller on torsional plant